NASA
Technical
Paper
2284

1985

Space Shuttle Orbiter Trimmed Center-of-Gravity Extension Study

Summary Report

William I. Scallion
and W. Pelham Phillips

Langley Research Center
Hampton, Virginia

NASA
National Aeronautics
and Space Administration

**Scientific and Technical
Information Branch**

SUMMARY

A summary of a study to determine removable aerodynamic modifications of the Space Shuttle orbiter that would extend the forward center-of-gravity (c.g.) trim capability has been presented. Aerodynamic, heat transfer, and system design studies determined that the most effective modifications were those that could replace all or a portion of the forward wing fillet. A forward-extended fillet provided an increase in forward c.g. trim capability of 1.9 percent of the reference body length. In-fillet canards increased the forward c.g. trim capability by the same amount, but the aft c.g. was limited by subsonic stability criteria. Two differently sized canards would be required to provide the same c.g. range as that provided by the forward-extended fillet. Both modifications increased the landed payload capability over that of the baseline orbiter.

INTRODUCTION

The longitudinal center-of-gravity range of the Space Shuttle orbiter for trimmed flight during entry, approach, and landing is quite limited. This puts a considerable constraint on the allowable mass distribution of Shuttle payloads being returned from orbit. In an effort to extend the orbiter center-of-gravity envelope, a study was undertaken at the Langley Research Center to determine the feasibility of developing simple "bolt-on" modifications to the aerodynamic shape. The major study guideline required that the resulting modifications would have a minimum impact on the baseline orbiter structure, subsystems, and thermal protection system. In general, this guideline was followed, but several concepts outside of these constraints which appeared to have some merit were also examined. Wind-tunnel force and moment tests (refs. 1 to 7) were conducted to assess the effectiveness of the modifications in extending the trimmed center-of-gravity envelope and to assess their influence on the vehicle entry flight characteristics. Aerodynamic heating tests and analyses (ref. 8) provided information on the impact of selected modifications on the thermal protection system requirements. Corresponding system design analyses were conducted to determine the structural weight penalties (ref. 9). This report is a summary of the study results for the modifications found to be the most effective in extending the orbiter trimmed center-of-gravity envelope.

SYMBOLS AND ABBREVIATIONS

The aerodynamic data are presented about the body system of axes, with only the lift coefficient presented about the stability axes. All aerodynamic data contained herein were nondimensionalized with the baseline model values of wing reference area, span, and mean aerodynamic chord. The moment reference point is located at 65 percent of the fuselage reference length aft of the model nose.

B_2, B_4, B_5 forebody modifications

b wing span

$C_{L,trim}$	trimmed lift coefficient
C_l	rolling-moment coefficient, $\frac{\text{Rolling moment}}{q_\infty S_{ref} b}$
C_{l_β}	$\frac{\partial C_l}{\partial \beta}$
C_m	pitching-moment coefficient, $\frac{\text{Pitching moment}}{q_\infty S_{ref} \bar{c}}$
C_N	normal-force coefficient, $\frac{\text{Normal force}}{q_\infty S_{ref}}$
C_n	yawing-moment coefficient, $\frac{\text{Yawing moment}}{q_\infty S_{ref} b}$
C_{n_β}	$\frac{\partial C_n}{\partial \beta}$
$C_{n_{\beta,dyn}}$	$C_{n_\beta} \cos \alpha - \frac{I_Z}{I_X} C_{l_\beta} \sin \alpha$
CFHT	Langley Continuous-Flow Hypersonic Tunnel
C_1, C_2	canards with fillet removed
C_3, C_4	in-fillet canards
$\bar{c}$	mean aerodynamic chord
c.g.	center of gravity
8-ft TPT	Langley 8-Foot Transonic Pressure Tunnel
fwd	forward
h	local heat-transfer coefficient
h_{ref}	heat-transfer coefficient to scaled 1-ft-radius sphere
I_X	moment of inertia about longitudinal body axis
I_Z	moment of inertia about normal body axis
KE	kinetic energy boundary based on design landing conditions
LTPT	Langley Low-Turbulence Pressure Tunnel

l	fuselage reference length
M	Mach number
M20He	22-inch aerodynamics leg of the Langley Hypersonic Helium Tunnel Facility
OMS	orbital maneuvering subsystem
q_∞	free-stream dynamic pressure
RCC	reinforced carbon carbon
RCS	reaction control system
R_l	free-stream Reynolds number based on l
S_{ex}	exposed area of modification
S_{ref}	theoretical wing reference area
S_1, S_2, S_3	fillet modifications
TPS	thermal protection system
20-in. M6	Langley 20-Inch Mach 6 Tunnel
UPWT	Langley Unitary Plan Wind Tunnel
V_{min}	minimum velocity
X_o, Y_o, Z_o	vehicle stations, full-scale orbiter coordinate system
x_{cg}	distance from model nose to center-of-gravity location
α	angle of attack
β	angle of sideslip
Δ	increment
δ_{BF}	body-flap deflection angle, positive trailing edge down
δ_e	elevon deflection angle, positive trailing edge down
δ_{SB}	split-rudder (speed brake) flare angle, positive trailing edges deflected outboard

OBJECTIVES AND APPROACH

The 140A/B Shuttle orbiter configuration showing the location of the payload bay and the forward and aft center-of-gravity (c.g.) locations that can be achieved with the baseline orbiter configuration is presented in figure 1. The Shuttle payload envelope in figure 2 shows the design payload weight and envelope of center-of-gravity locations with respect to the forward end of the payload bay. The left-hand

boundary represents the design forward payload c.g. limit for a given payload weight. The intersection of the horizontal line representing the entry design payload limit of 32 000 lb with the forward control boundary designates the subsonic design point of the orbiter (V_{min} ≈ 169 knots, $\alpha \approx 15°$ at standard sea-level conditions for an orbiter landing weight of 188 000 lb including the entry design payload). The cross-hatched area represents the weights and c.g. locations of several early payloads considered for the Shuttle; and, as can be seen, this area is outside the design payload envelope. The objective of the study reported herein was to define configuration modifications which would extend the forward payload c.g. boundary to include additional payloads of this type.

The capabilities of the orbiter braking system can be equated to the maximum kinetic energy level at landing. This kinetic energy limit creates another constraint on the allowable c.g. locations. The boundary associated with the kinetic energy limitation was chosen for the mass and velocity values of the aforementioned subsonic design point. This boundary is designated as the landing kinetic energy boundary and is also shown in figure 2. The boundary shown does not represent the absolute upper limit of the landing-gear system (struts, tires, and brakes) as designed, but it was chosen in this study as an upper limit for the vehicle with modifications designed to extend the forward payload boundary. The allowable payload is decreased by this boundary as payload center-of-gravity moves forward, and a desirable effect of modifications to extend the forward payload boundary would be to also shift the kinetic energy boundary upward; i.e., to permit lower landing speeds.

An assessment of the orbiter fore and aft c.g. control boundaries is shown as a function of Mach number in figure 3. The orbiter design c.g. range is also shown on this figure. The forward c.g. limit represented by the line at 0.65 reference body length was used to derive the forward payload boundary shown in figure 2.

Control boundaries are defined differently for the most forward and most aft c.g. cases. For the most forward c.g. case, the boundary is defined such that at a trimmed flight condition on the control boundary, the capability exists to generate a ΔC_m margin by deflecting the elevons to a full up position (-40°). A ΔC_m value of 0.015 is used below Mach 10, and above this Mach number, a value of 0.020 is specified. For the most aft c.g. case, the boundary is defined by the ability to trim the orbiter with a maximum elevon deflection of +10.0°. A margin of 5° down elevon is available with this definition. Both forward and aft c.g. control margin definitions allow for roll control requirements and aeroelastic effects. In addition, the foregoing trim capabilities were required to be viable for an angle-of-attack increment of 4° above and below the nominal trim angle of attack for a given Mach number along the entry trajectory. Note that the forward c.g. control boundary is extremely close to the design c.g. line in the Mach number range between 4 and 6, and any forward extension of the control boundary would require aerodynamic modifications that would be highly effective in this speed range.

The approach taken for this study was to derive a set of possible modifications and to utilize available orbiter models to conduct preliminary wind-tunnel tests. The study ground rules specified that the modifications were to have a minimum impact upon the baseline orbiter structure, weight, and TPS. The preferable approach to meeting these requirements was to make the modifications removable (in the form of retrofit conversion kits) so that the baseline orbiter could be flown when the additional trimmed c.g. capability was not needed. The main thrust of the study adhered to this approach; however, in the early part of the study, many other modifications were examined, some in detail, and others only briefly. Concurrently with the wind-tunnel testing, preliminary system design studies were conducted to determine the

system weights and impact upon the orbiter structure. The preliminary wind-tunnel tests were used to narrow the set of modifications to those that were considered to be the most promising. In several instances, completion of preliminary designs before wind-tunnel tests resulted in fairly detailed designs of modifications that were later found to be unacceptable. Some of these designs are included to portray the scope of the study.

The potential configuration changes examined during the study are shown in figure 4. The forebody modifications shown on the left of figure 4 consisted of changes in the forebody chamber, length, and width and utilization of the nose gear doors as hypersonic trim flaps. All these modifications were expected to provide a nose-up trim increment in the Mach number range of 4 to 6; however, they would not be expected to contribute additional trim at transonic and subsonic speeds. (See ref. 2.) Although sufficient forward c.g. trim capability is available at subsonic speeds, the additional elevon trim requirement would result in an accompanying reduction in lift and an increase in the landing speed. Where the increases in forward c.g. trim requirements are small, the associated subsonic trim lift losses could probably be tolerated, but larger trim requirements would have to be accompanied by modifications that minimized the lift loss due to trim. One such modification envisioned was the extended-span body flap, shown in the lower left-hand side of figure 4, which had a longer moment arm than the elevons and would be expected to incur proportionately smaller lift decrements due to trim.

The changes in fillet geometry considered during the study are shown on the right-hand side of figure 4. The fillets were envisioned to be completely removable so that the baseline fillet could be replaced by a modified fillet for entries in which a forward vehicle center of gravity was planned. The fillets would be expected not only to increase the hypersonic nose-up trim capability, but also to increase the low-speed trim capability.

The left-hand fillet modification provided increased lifting area by increasing the span of the fillet. In addition to the interface between the fillet and fuselage, some modification to the wing leading edge would be required. The right-hand fillet modification was designed to shift the additional lifting area forward on the forebody. To accommodate the forward portion of the fillet, some structural modification of the forebody would be required. Several candidate canard configurations designed to fit in the forward fillet area as shown in figure 4 were also studied. Once the trends in the modifications were established, a single, detailed model was constructed so that a consistent set of data for the more promising modifications could be obtained.

Although this study emphasizes the effects of the modifications on the entry flight characteristics of the orbiter, studies of the effects of the modifications on the launch configuration would be required for a complete evaluation of the chosen application.

APPARATUS, CONFIGURATIONS, AND SUPPORTING TESTS

Apparatus

Six orbiter wind-tunnel models were used during the study. Pertinent dimensions and full-scale body stations of three of these models are shown in figures 5, 6, and 7. The model dimensions and body stations are given in inches. A comparison of similar body stations shows that the modifications differed slightly from model to

model. The dimensions and stations shown represent measurements of the models that were made subsequent to construction. Preliminary force investigations of a parametric nature were conducted with an existing 0.015-scale 140A/B orbiter model (fig. 5) and an existing 0.01-scale orbiter model. Later investigations were conducted with an existing 0.004-scale 139B orbiter model (fig. 6) and with a 0.01-scale 140A/B model (fig. 7) constructed specifically for this study. Photographs of these two force models are shown in figures 8 and 9. Three 0.01-scale filled epoxy models were also constructed for aerodynamic heating investigations on the effects of the more pertinent modifications, and a photograph of these models is presented in figure 10.

Configurations

Most of the configurations were initially investigated with the 0.015-scale and 0.004-scale models shown in figures 5 and 6, respectively. Three forebody shapes, B_2, B_4, and B_5 (fig. 5(c)), were investigated. A simple change in forebody camber in which the cross sections ahead of station 400 were moved upward without changing the cross-sectional shape is designated as the minimum camber forebody, B_2. The other two forebodies, B_4 and B_5, were constructed with increases in width, length, and negative camber. Details of the nose-gear-door trim flap and the extended-span body flap are shown in figure 5(b).

Two fillet modifications, S_1 and S_3 (figs. 5(a) and 6), consisted of an increase in span over that of the baseline. Both fillets originate at the same forward body station as the baseline fillet, and the increase in span was obtained by decreasing the leading-edge sweep from the forward intersection with the body. Most of the area increase resulting from this type of planform change was centered on the aft portion of the fillet. The third fillet modification, S_2, resulted from an attempt to shift the additional lifting area forward and thus provide a more effective moment arm. This fillet extended further forward on the forebody (to station 300) than the baseline fillet. In order to accommodate the forward portion of the fillet, some structural modification to the forebody would be required in addition to the area exposed by removal of the baseline fillet.

Several candidate canard configurations designed to fit in the forward fillet area as shown in figure 4 were also studied. Details of the several canards are shown in the sketches in figure 5. Early in the study, the Space Shuttle Program Office requested that a canard designed to replace the entire fillet be examined. Two canards, C_1 and C_2, shown in figure 5(a), were designed for this purpose. It was believed that a canard designed to replace only the forward portion of the fillet would be a simple approach toward providing increased forward c.g. trim capability. Two flat plate canards, C_3 and C_4, shown in figures 6 and 7(a), were constructed to give a range of canard sizes and, therefore, trim effectiveness. The blended canard shown in figure 7(a) was about the same size as the large flat plate canard, C_4, and was designed more realistically for the actual flight environment where loads and aerodynamic heating effects must be considered.

Tests

The wind-tunnel tests were conducted in two phases over a Mach number range from 0.25 to 20.3 in several facilities. The first phase consisted of preliminary tests in the Langley Unitary Plan Wind Tunnel to obtain data on the proposed modifications

with the 0.015-scale model at a Mach number of 4.6 (near the critical longitudinal trim Mach number range) to determine their effectiveness. With the exception of the data that are presented herein, none of those data were published. The second phase consisted of tests with a single model (0.01-scale) across the Mach number range of 0.25 to 10.3. The more applicable modifications were tested on this model to obtain a consistent set of results across the speed range. An exception to this approach was the investigation conducted at Mach 20.3 in the 22-inch aerodynamics leg of the Langley Hypersonic Helium Tunnel Facility, where a much smaller model was required. The 0.004-scale model (fig. 9) was used in these tests. The heat-transfer data were obtained by using the phase-change coating technique and the models shown in figure 10. The same models were used in oil-flow studies to examine the surface flow and separation and reattachment regions on the upper surface of the body and wings. These tests and techniques are reported in reference 8.

The wind-tunnel tests conducted in this study are listed in the following table, which indicates the test facility and the reference in which the data are published, if applicable.

SUPPORTING TESTS FOR ORBITER c.g. STUDY

Langley facility	Mach number	Model scale	Modifications studied	Source
LTPT	0.25	0.015	Wing position fillet, wing-tip extension, and body-flap geometry	Preliminary data (unpublished)
8-ft TPT	0.35 to 1.2		Body-flap geometry, fillet geometry, and canard	
UPWT	2.5 to 4.6		Forebody geometry, fillet geometry, canard, and nose-gear-door trim flap	
CFHT	10.3	.01	Forebody, body-flap geometry, and nose-gear-door trim flap	
LTPT	0.25		Fillet, forebody, and canard	Reference 1
8-ft TPT	0.35 to 1.2		Fillet, forebody, and canard	Reference 2
UPWT	1.5 to 4.6		Fillet, forebody, and canard	References 3 and 4
20-in. M6	6.0		Fillet, forebody, and canard	Reference 5
CFHT	10.3		Fillet, forebody, and canard	Reference 6
M20He	20.3	.004	Fillet, forebody, and canard	Reference 7
CFHT	10.3	.004	Fillet and canard (heat transfer)	Reference 8

RESULTS AND DISCUSSION

Preliminary Aerodynamic Characteristics

As mentioned previously, preliminary aerodynamic studies were conducted at supersonic speeds (Mach 2.5 to 4.6) with the 0.015-scale model shown in figure 5. These study results were used to determine the trim effectiveness of the candidate modifications in the speed range where longitudinal trim was considered marginal. Additional tests were conducted to determine the subsonic trim characteristics of the various modifications.

Effect of forebody modifications.- The forward and aft trimmed c.g. locations normalized to body length (x_{cg}/l) for the forebody configurations are shown in figure 11 as they vary with Mach number. As can be seen, minor changes in the forebody camber alter the supersonic longitudinal trim. Increases in forebody length, width, and camber (B_4 and B_5, fig. 5(c)) provided increases in forward c.g. trim capability by as much as 1.4 percent of the body length as shown by the diamond symbols representing the maximum combination tested (B_4). It was assumed that the forebodies would not provide low-speed trim effectiveness (substantiated in ref. 2) to maintain the baseline landing kinetic energy level, and that additional subsonic trim capability could be obtained by extending the span of the body flap at subsonic speeds.

The subsonic effectiveness of the body-flap extension is presented in figure 12. As can be seen, the span extension essentially doubled the effectiveness of the body flap. This would enable the body flap to trim a much more forward c.g. location at the nominal angle of attack of 15°; however, the trim lift would be reduced below the nominal. The loss in lift can be restored by deflecting the elevons downward as flaps, but the additional negative moment would have to be compensated for by the body flap, and the net available forward c.g. trim capability would therefore be reduced. A calculation of the trim capability for the extended-span body flap without reducing the trim lift from the baseline value resulted in a net increase in forward c.g. trim capability of 0.48 percent of the reference body length. This value was 37 percent of the additional supersonic trim capability indicated by the maximum width forebody in figure 11.

Another modification for which preliminary data were obtained was a nose-gear-door trim flap. The effects of this modification on the longitudinal characteristics of the orbiter at Mach numbers of 2.5 and 4.6 are shown in figure 13. The flap increased the out-of-trim pitching-moment coefficient at both Mach numbers, primarily because the deflected flap induced separation on the underside of the forebody and thereby decreased the nose-up loading in this area.

Effect of fillet modifications.- The effect of increasing the forward fillet area on the orbiter supersonic trim capability is shown in figure 11. All three fillets tested increased the forward c.g. trim capability of the orbiter, but the fillet with area extended forward around the forebody (S_2) was the most effective. The additional increment was about 2.5 percent of the body length. All three fillets tended to increase the subsonic longitudinal trim capability and the trim lift of the orbiter. The forward c.g. trim capability of the orbiter with the fillets at subsonic speeds is greater than that at supersonic speeds, and the trim lift is sufficient to reduce the landing speeds below that of the baseline configuration. As shown by figure 14, the most effective fillet at subsonic speeds was the largest one with extended span (S_3). The decreased sweep of this fillet increased the overall lift effectiveness of the orbiter wing.

Effect of canards.- The results of the preliminary studies of the supersonic trim effectiveness of the three canard configurations shown in figure 5(a) are presented in figure 11. Canards C_1 and C_2 were tested with the baseline fillet removed and the basic wing leading edge faired into the body. Both canards exhibited supersonic longitudinal trim effectiveness equal to or slightly better than the baseline fillet; however, neither canard produced a significant increase in supersonic trim capabilities. The third canard, C_3, was tested in conjunction with the baseline fillet, and as can be seen in figure 11, produced an additional increment in forward c.g. trim effectiveness of about 1.8 percent of the reference body length.

The subsonic longitudinal characteristics of the orbiter with the C_1 and C_3 canards are shown in figure 15. Both canards can provide greater trim capability at subsonic speeds than at supersonic speeds, but the longitudinal instability of the C_1 canard configuration would exceed the constraint on subsonic stability as specified by the design requirements (2-percent negative static margin). Although the stability of the in-fillet canard configuration (C_3) appears to be about the same as that of the C_1 canard, the c.g. for the C_3, because of its greater hypersonic trim capability, would be further forward than the moment center ($x_{cg}/l = 0.65$) for which the aerodynamic data are presented. With the center of gravity shifted forward 1.8 percent of the body length (corresponding to the most forward hypersonic trim c.g., fig. 11), the subsonic static margin of the orbiter with the in-fillet canard would be about -1.1 percent l at $\alpha = 2°$, but would be zero or greater for angles of attack above 10°.

Summary Aerodynamic Characteristics

The preliminary aerodynamic studies indicated that the most effective modifications for extending the hypersonic forward c.g. trim capability of the orbiter were the forward-extended fillet and the in-fillet canards C_3 and C_4 (fig. 7(a)). The aerodynamic characteristics of the orbiter as obtained from tests of the 0.01-scale model with the forward-extended fillet (S_2) and the in-fillet canards (C_3 and C_4) (refs. 1 to 7) are presented in figures 16, 17, and 18. Figure 16 presents the forward control boundaries of the baseline model, the model with the in-fillet canards, and the forward-extended fillet. The most effective modification in the Mach number range of 4 to 6 was the large flat plate in-fillet canard (C_4). This configuration, however, is not considered to be realistic in view of the heating environment that would be encountered at hypersonic speeds. Limited data were obtained at Mach 1.5, 2.0, 2.5, and 6 on the blended canard. These data are represented by the right triangular symbols on the figure. As can be seen, the blended canard is less effective than the flat plate canard at $M = 6$. Posttest measurements of the canard models indicated that although the areas of the two canards were nearly the same, the effective moment arm of the blended canard was noticeably shorter than that of the flat plate canard. The blended canard as tested is only slightly more effective as a hypersonic trimmer than the forward-extended fillet.

The subsonic longitudinal trim characteristics of the 0.01-scale orbiter model with the forward-extended fillet and the canards are compared with those of the baseline model in figure 17. This figure presents the variation of subsonic $C_{L,trim}$ with center-of-gravity location for the design landing angle of attack of 15°. The solid circular symbol on the baseline curve represents the baseline subsonic design point. The boundaries shown indicate the maximum forward hypersonic trim c.g. (left-hand boundary) and the aft subsonic static stability margin (right-hand boundary). As can be seen, the widest trim center-of-gravity range can be obtained with the forward-extended fillet modification (S_2). The canards can provide approximately the

same hypersonic forward c.g. trim capability, but because the high subsonic lift-curve slope (Aspect ratio = 1.79) causes an increase in the overall subsonic instability, the aft c.g. location is limited by the static-stability-margin constraint to locations much further forward than those for the forward extended fillet. Because of this, no single canard can provide the same trimmed c.g. range as the fillet. Separate canards, each designed for a portion of the c.g. range, would be required to cover the same c.g. range as the fillet. The canards do provide somewhat higher trim lift capability than the fillet modification, and all the modifications exceed the baseline trim lift capability.

The variation of the lateral-directional parameter $C_{n_{\beta,dyn}}$ with Mach number for the baseline orbiter model and the model with the forward-extended fillet and canard modifications is shown in figure 18. Although a positive value of $C_{n_{\beta,dyn}}$ does not constitute a sufficient condition to guarantee positive lateral-directional stability, the data on the figure herein provide comparisons of the effectiveness of the modifications with the baseline configuration. In general, the values of $C_{n_{\beta,dyn}}$ for the orbiter with modifications are higher than those for the baseline and indicate that the lateral-directional characteristics are comparable with or slightly better than those of the baseline configuration.

Heat-Transfer Studies

Heat-transfer studies (ref. 8) were conducted at Mach 10.3 on 0.01-scale orbiter models representing the baseline vehicle, the forward-extended-fillet configuration (S_2), and the orbiter with the blended canard (fig. 10). Surface oil-flow studies were also conducted. In general, the results from reference 8 indicated that no significant adverse effects on the lower-surface heating were produced by the addition of the modifications. Typical results from this reference are shown in figure 19. As can be seen in figure 20, the extended-fillet configuration had a considerably smaller interference heating pattern than the baseline, whereas the blended-canard configuration provided a longer interference heating pattern on the body sides and the OMS pod. The surface oil-flow patterns on the three configurations (ref. 8) are shown in figure 21.

The following table taken from reference 8 gives the additional side thermal protection system weights for the extended-fillet and blended-canard configurations.

INCREMENTAL TPS SIDE WEIGHTS TO ACCOMMODATE MODIFICATIONS

Configuration	TPS weight - baseline TPS weight, lb		
	$\alpha = 30°$; $R_l = 1 \times 10^6$	$\alpha = 30°$; $R_l = 2 \times 10^6$	$\alpha = 40°$; $R_l = 1 \times 10^6$
Baseline	0	0	0
S_2 fillet	184	51	9
Blended canard	176	176	144

These incremental side weights were obtained from comparison of the baseline TPS weight with the weight of a TPS designed for the highest heating resulting from the combination of the heating distributions for the retrofit (fillet or canard) and baseline configurations. The orbiter TPS design trajectory was used to derive these weights. The resulting weight increases shown in the table are the "scar" weights that the baseline orbiter must carry to accommodate entry heating on the sides with the respective retrofit configuration. In comparison with the structural weights of the modifications (discussed in a following section), the additional thermal protection system weights required by the modifications are relatively small.

Systems Design Studies

As stated previously, system design studies of the modifications were conducted concurrently with the aerodynamic investigations. The results of these studies are reported in reference 9 and are summarized herein.

The impact of a simple change in forebody camber ahead of the cabin pressure vessel (B_2) on the system design is shown in figure 22. This change corresponds to the modification of figure 5(c). The major impact would consist of changes in the nose-landing-gear linkage and attachment, and, as stated in reference 9, if the changes were incorporated during initial construction, the weight penalty would be approximately 50 lb. Increasing the forebody length, width, and camber to correspond to forebody B_4, shown in figures 5(c) and 7(b), by retrofitting to the baseline forebody would increase the orbiter dry weight by about 1104 lb. In addition, the orbiter with the retrofitted maximum width forebody would require the two-position body-flap span extensions in figure 23 to maintain trim without increasing landing speeds. The weight penalty for this modification was estimated to be 1336 lb.

Modifications to the wing forward-fillet area were considered to be the most promising because a variety of modifications such as revised fillet shapes and canards could be attached to this area. The scar weight penalties for making the baseline fillet removable are shown in figure 24. Removal of the baseline fillet reduced the weight of the orbiter by 1647 lb (ref. 9). Figure 25 shows that replacement of the baseline fillet with the forward-excended fillet, S_2, increased the vehicle weight by 1037 lb with a corresponding overall vehicle c.g. shift forward of 0.1 percent of the body length. It must be noted that the system impact study of reference 9 did not include a scar weight provision for attaching this fillet to the forebody ahead of station 534. The incremental weights of the fillets with increased span (fig. 5(a)) were estimated to be 432 lb for S_1 and 955 lb for S_3. A fairly detailed preliminary design study of the blended canard was conducted and presented in reference 9. Figure 26 illustrates the structural arrangement, and figure 27 shows the overall systems impact of the canard. This canard was designed to utilize the total length exposed by removing portions of the baseline fillet between stations 534 and 807 (an existing manufacturing interface). The weights of smaller canards were obtained by proportionally scaling the weights resulting from the preliminary design. Two deployable canards (fig. 28) were also studied in reference 9. These systems would result in permanent weight increases, since they would be carried on all flights. No aerodynamic investigations were conducted on the deployable canards.

SYNTHESIS

The aerodynamic, heating, and system design study results were discussed independently in the previous section; however, a proper assessment of the overall effectiveness of the various modifications requires that the separate results be considered as a whole. The results indicate that from the standpoint of performance and ease of retrofit, the most promising modifications are those that could replace all or a portion of the baseline forward wing fillet. These modifications were narrowed to the forward-extended fillet and in-fillet canards in the final aerodynamic and heat-transfer studies.

The effects of the weights of the modifications on the orbiter c.g. were combined with the aerodynamic effect of the modifications on the effective center of pressure to determine the actual allowable trim c.g. range. Once this was determined, the maximum forward and aft c.g. values were used to calculate a payload-bay envelope for each of the modifications. Additionally, the subsonic design-point value of landing kinetic energy was used to determine payload weight boundaries for each of the modifications.

For the forward-extended fillet, the procedure was relatively straightforward. The canard, although capable of providing somewhat greater hypersonic trim capability, was severely limited in aft c.g. locations by the subsonic stability-margin criteria. As mentioned previously in the discussion of figure 17, no single canard can provide the same trimmed c.g. range as the extended fillet. Figure 29, derived from the aerodynamic data for the C_3 and C_4 canards, was used to determine the size and number of separate canards required to provide about the same c.g. range as the fillet. Two canards, designated A and B on the figure, are sized to provide a comparable c.g. range when their respective c.g. ranges are added. The canards would have to be interchanged for each flight to provide the required c.g. range. Although the trim ranges of the canards do not appear to overlap in figure 29, they form a continously overlapping trimmed c.g. range when the effects of installation and scar weights on the vehicle c.g. are included. The weights of the canards were scaled from the weight of the blended canard of figure 27. The summary weights and forward c.g. capabilities of the S_2 fillet and canards A and B are presented in table I.

The resulting payload-bay envelopes for the forward-extended fillet and the canards are compared with the baseline orbiter in figure 30. In this figure, the baseline orbiter weight was updated to the average empty weight of the orbiter used for the first five flights, which is approximately 186 000 lb. The resulting baseline payload-bay envelope is shown in figure 30 as the dashed line. The original design payload-bay envelope is also shown in the figure as the solid line. Note that the effect of increased orbiter empty weight is to increase the size of the baseline payload-bay envelope. That is, the heavier orbiter is less sensitive to payload c.g. location. The baseline landing kinetic energy curve shown in figure 30 is also updated to reflect the more realistic flight orbiter weight plus the design entry payload weight of 32 000 lb, resulting in a total landed weight of 218 000 lb.

As shown in figure 30, of the modifications considered, the forward-extended fillet, S_2, produced the largest payload-bay-envelope extension. At the design entry payload weight, the c.g. ranged from station 7.5 to station 28.5, which overlapped the baseline forward c.g. boundary by a small amount. The forward boundary at station 7.5 represents a forward extension of the orbiter hypersonic trimmed c.g. capability of 1.9 percent of the reference body length, as shown in table I. Note also that the landing kinetic energy boundary was moved upward by this modification. This represents an average increase in landed payload capability of 14 506 lb.

In-fillet canards increased the forward c.g. trim capability by 1.9 percent, but the aft c.g. was limited by the subsonic instability of the configuration. The canard modifications A and B also provide increased landed payload capability (about 20 000 and 11 000 lb, respectively); however, the combined ranges of canards A and B are required to cover essentially the same trimmed c.g. range as the extended fillet. This indicates that the canard modification is not as aerodynamically suitable as the extended fillet. The canards, therefore, would not have the same operational flexibility as the extended fillet, in that more between-flight configurational changes would have to be made to cover the same payload c.g. range. On the other hand, installation of the canards would be a much simpler task because the removal and replacement area as confined between stations 534 and 807, an established manufacturing interface. The extended fillet would require removal of the entire baseline fillet plus an additional area around the forebody where no current manufacturing interface exists. The impact of providing for retrofit in this area was not studied in reference 9, nor has the impact of the presence of the fillet on the existing forward RCS and air data systems been established. A trade-off between the complexities of retrofitting the extended fillet, the simplicity of mounting the canards, and the overall resulting operational flexibility of each system would be required to establish which would be more applicable.

CONCLUDING REMARKS

Aerodynamic, heat-transfer, and system design studies conducted to determine configuration modifications to the Space Shuttle orbiter that would extend its forward center-of-gravity (c.g.) trim capability have been summarized. The most effective modifications were those that could replace all or a portion of the forward wing fillet. Of these modifications, the forward-extended fillet provided the widest trimmed center-of-gravity range and the most forward trimmed center-of-gravity capability, an increase of 1.9 percent over that of the baseline configuration. In-fillet canards increased the forward center-of-gravity trim capability by 1.9 percent, but the aft c.g was limited by the subsonic instability of the configuration. Two canards of different size would be required to provide a center-of-gravity range similar to that of the forward-extended fillet. Both fillet and canard modifications provided increased landed payload capabilities over that of the baseline orbiter. Further study will be required to establish if the simplicity of the canard retrofit would outweigh the greater performance of the fillet with its attendant installation complexity.

Langley Research Center
National Aeronautics and Space Administration
Hampton, VA 23665
February 12, 1985

REFERENCES

1. Phillips, W. Pelham: Space Shuttle Orbiter Trimmed Center-of-Gravity Extension Study: Volume VII - Effects of Configuration Modifications on the Subsonic Aerodynamic Characteristics of the 140A/B Orbiter at High Reynolds Numbers. NASA TM-72661, Vol. VII, 1981.

2. Phillips, W. Pelham: Space Shuttle Orbiter Trimmed Center-of-Gravity Extension Study: Volume II - Effects of Configuration Modifications on the Aerodynamic Characteristics of the 140A/B Orbiter at Transonic Speeds. NASA TM X-72661, Vol. II, 1976.

3. Phillips, W. Pelham; and Fournier, Roger H.: Space Shuttle Orbiter Trimmed Center-of-Gravity Extension Study: Volume IX - Effects of Configuration Modifications on the Aerodynamic Characteristics of the 140A/B Orbiter at Mach Numbers of 1.5, 2.0, and 2.5. NASA TM-72661, Vol. IX, 1985.

4. Phillips, W. Pelham; and Fournier, Roger H.: Space Shuttle Orbiter Trimmed Center-of-Gravity Extension Study: Volume V - Effects of Configuration Modifications on the Aerodynamic Characteristics of the 140A/B Orbiter at Mach Numbers of 2.5, 3.95 and 4.6. NASA TM-72661, Vol. V, 1979.

5. Phillips, W. Pelham: Space Shuttle Orbiter Trimmed Center-of-Gravity Extension Study: Volume VIII - Effects of Configuration Modifications on the Aerodynamic Characteristics of the 140A/B Orbiter at a Mach Number of 5.97. NASA TM-72661, Vol. VIII, 1984.

6. Bernot, Peter T.: Space Shuttle Orbiter Trimmed Center of Gravity Extension Study: Volume I - Effects of Configuration Modifications on the Aerodynamic Characteristics of the 140A/B Orbiter at Mach 10.3. NASA TM X-72661, Vol. I, 1975.

7. Scallion, William I.; and Stone, David R.: Space Shuttle Orbiter Trimmed Center-of-Gravity Extension Study. Volume IV - Effects of Configuration Modifications on the Aerodynamic Characteristics of the 139B Orbiter at Mach 20.3. NASA TM X-72661, Vol. IV, 1978.

8. Dunavant, James C.: Space Shuttle Orbiter Trimmed Center-of-Gravity Extension Study. Volume III - Impact of Retrofits for Center-of-Gravity Extension on Orbiter Thermal Protection System. NASA TM-72661, Vol. III, 1979.

9. MacConochie, Ian O.: Space Shuttle Orbiter Trimmed Center of Gravity Extension Study. Volume VI - System Design Studies. NASA TM-72661, Vol. VI, 1978.

TABLE I.- SUMMARY CHARACTERISTICS OF SELECTED MODIFICATIONS

Configuration	Modification weight increment, lb	Structural scar weight, lb	TPS scar weight, lb	Baseline empty weight, lb	Installed empty weight, lb	$\Delta x_{cg}/l$		
						Aerodynamics	Weight	Net[a]
Baseline	0	0	0	186 000	186 000	0	0	0
S_2 fillet	[b]1037	[b]111	[b]184	186 295	187 332	0.0201 fwd[c] .0280 fwd[d]	0.0011 fwd .0011 fwd	0.0190 fwd[c] .0269 fwd[d]
Canard A	2085	40	184	186 224	188 309	.0231 fwd[c] .0310 fwd[d]	.0038 fwd .0038 fwd	.0193 fwd[c] .0272 fwd[d]
Canard B	1033	40	184	186 224	182 257	.0111 fwd[c] .0190 fwd[d]	.0019 fwd .0019 fwd	.0092 fwd[c] .0171 fwd[d]

[a]Aerodynamics minus weight.
[b]Does not include scar weight for forebody area.
[c]Actual wind-tunnel increments (x_{cg}/l for baseline model - x_{cg}/l for modification).
[d]Increment based upon design forward x_{cg}/l (0.6500 - x_{cg}/l for modification).

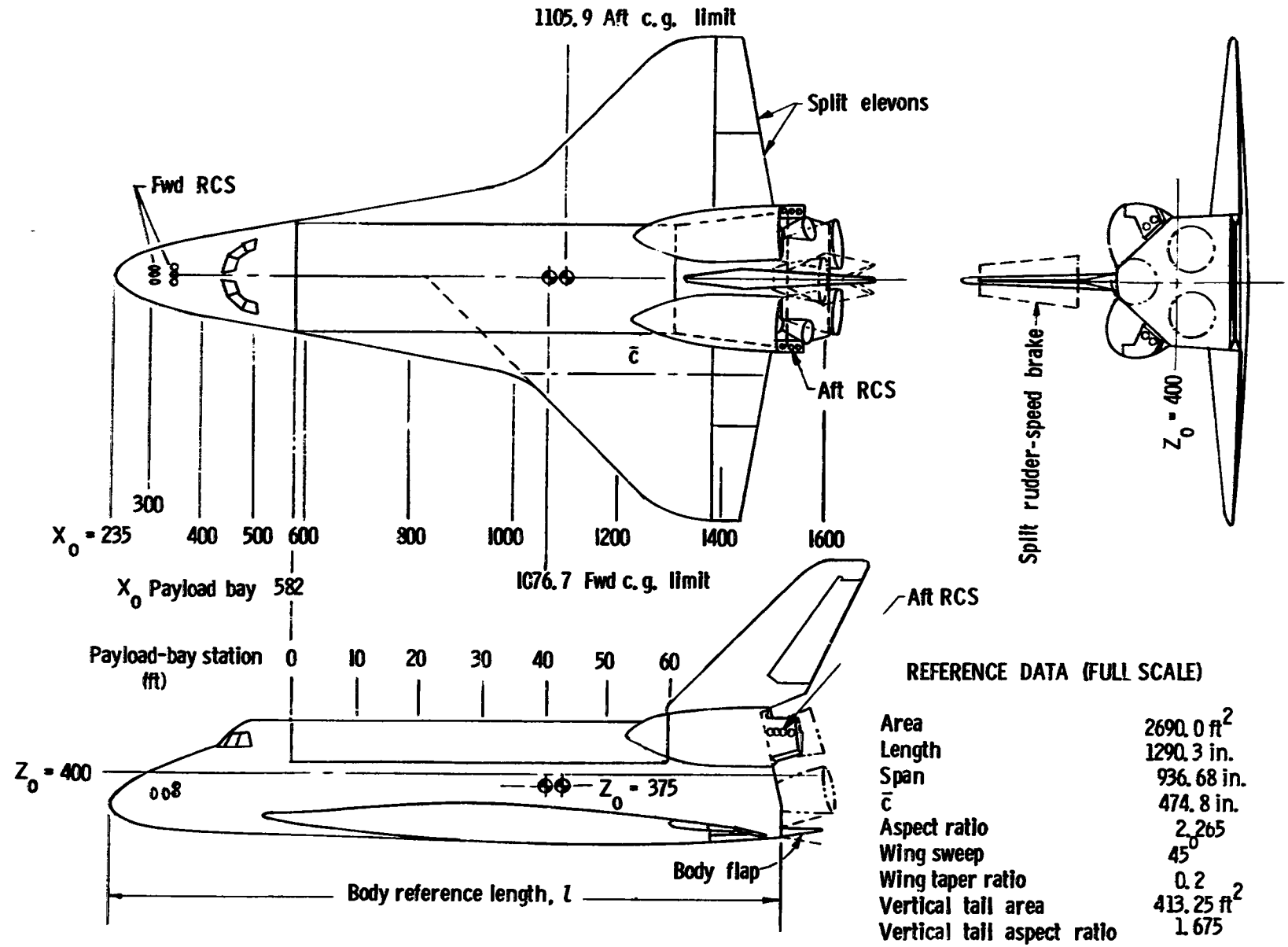

REFERENCE DATA (FULL SCALE)

Area	2690.0 ft^2
Length	1290.3 in.
Span	936.68 in.
$\bar{c}$	474.8 in.
Aspect ratio	2.265
Wing sweep	45^0
Wing taper ratio	0.2
Vertical tail area	413.25 ft^2
Vertical tail aspect ratio	1.675

Figure 1.- Shuttle orbiter 140A/B configuration. Station locations are in inches unless otherwise specified.

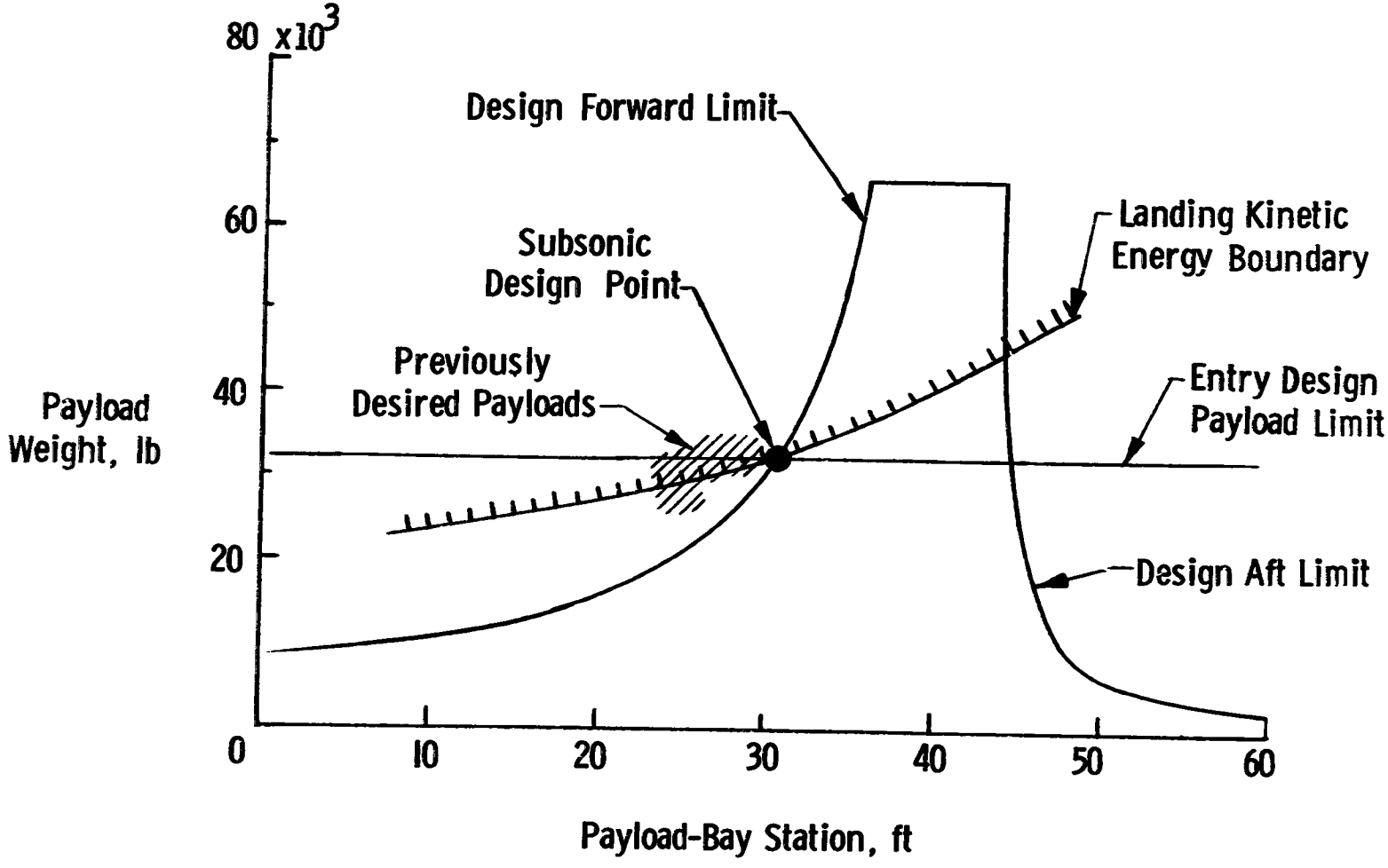

Figure 2.- Baseline orbiter payload c.g. envelope.

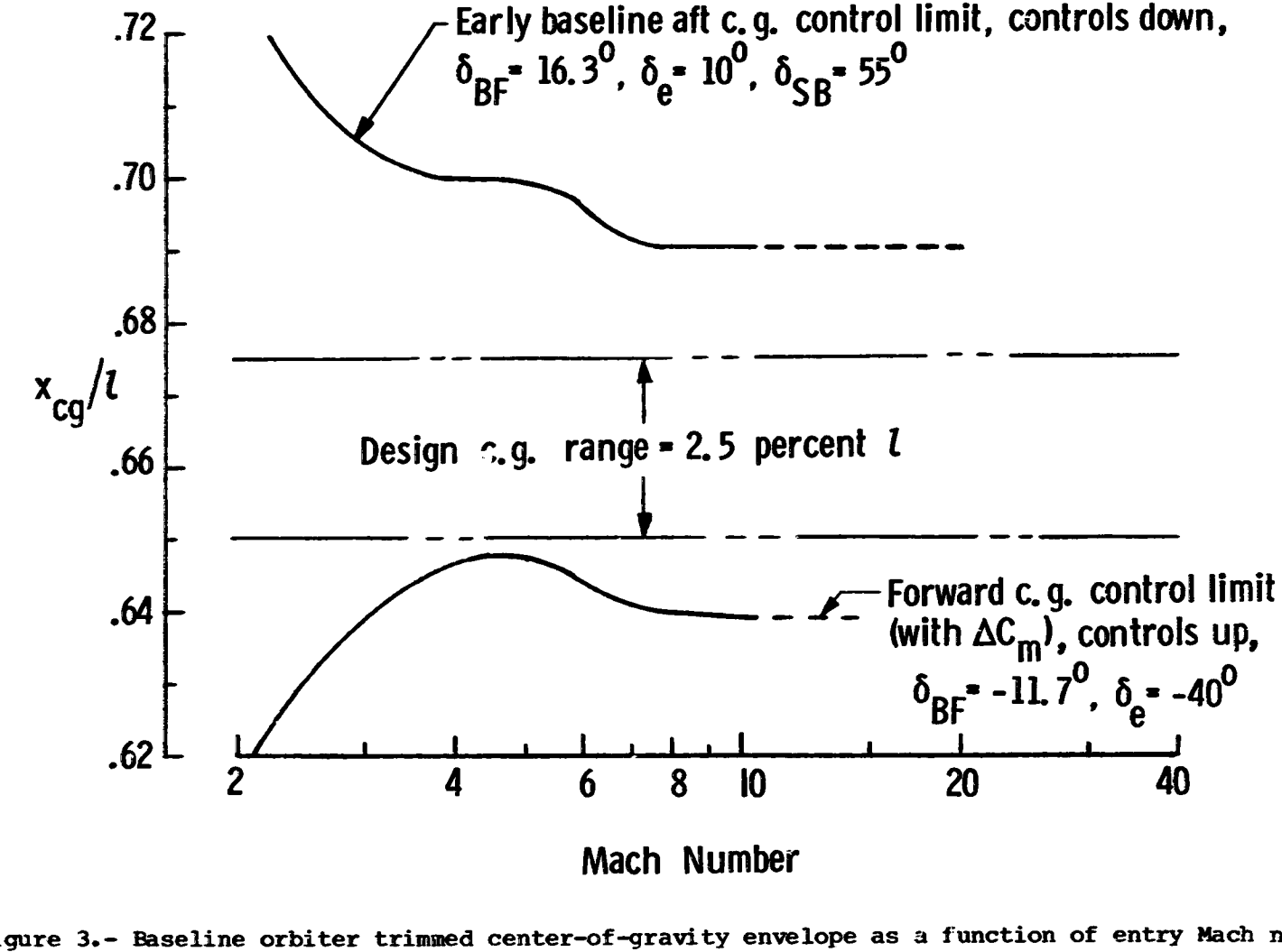

Figure 3.- Baseline orbiter trimmed center-of-gravity envelope as a function of entry Mach number.

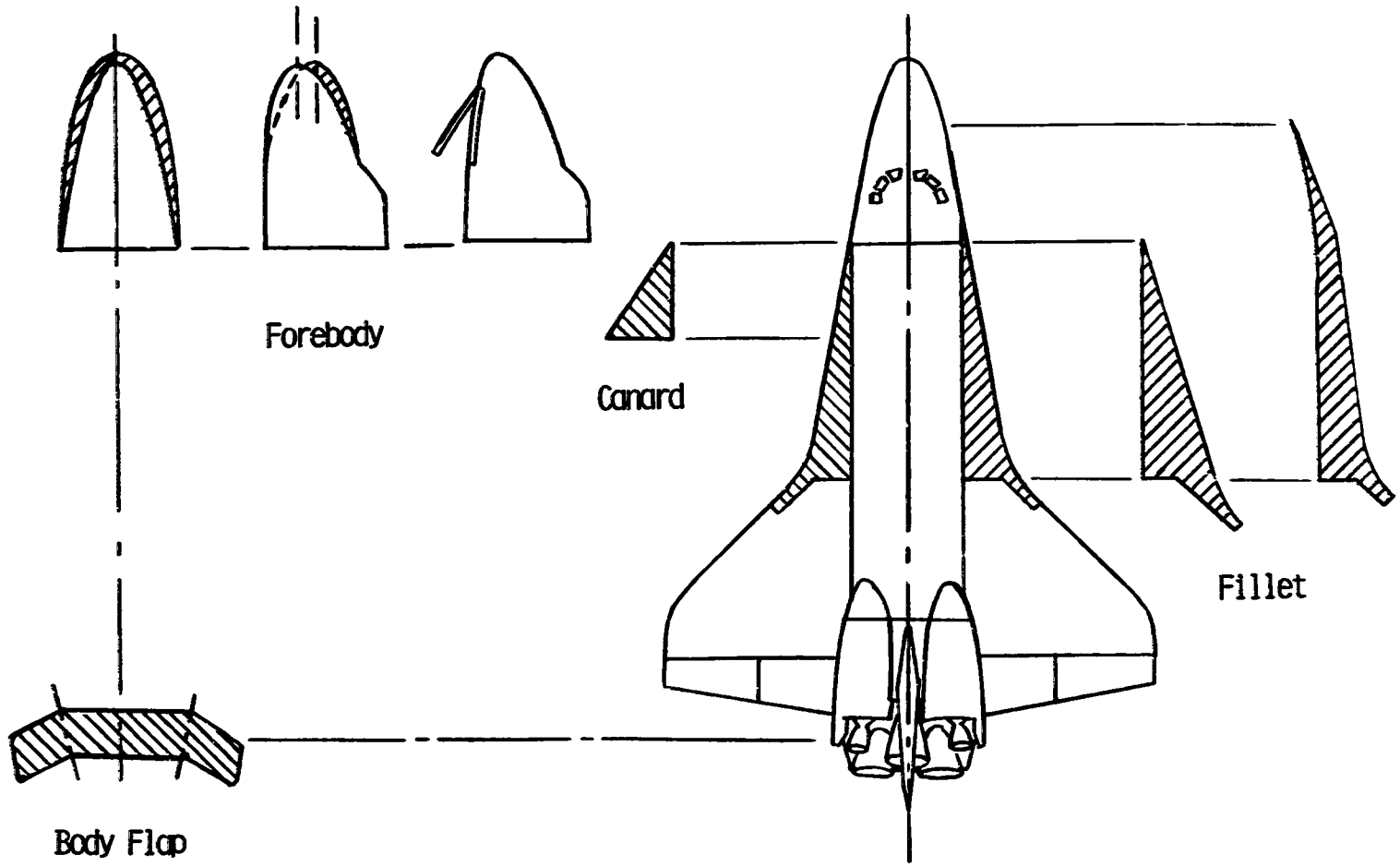

Figure 4.- Potential configuration changes examined during study.

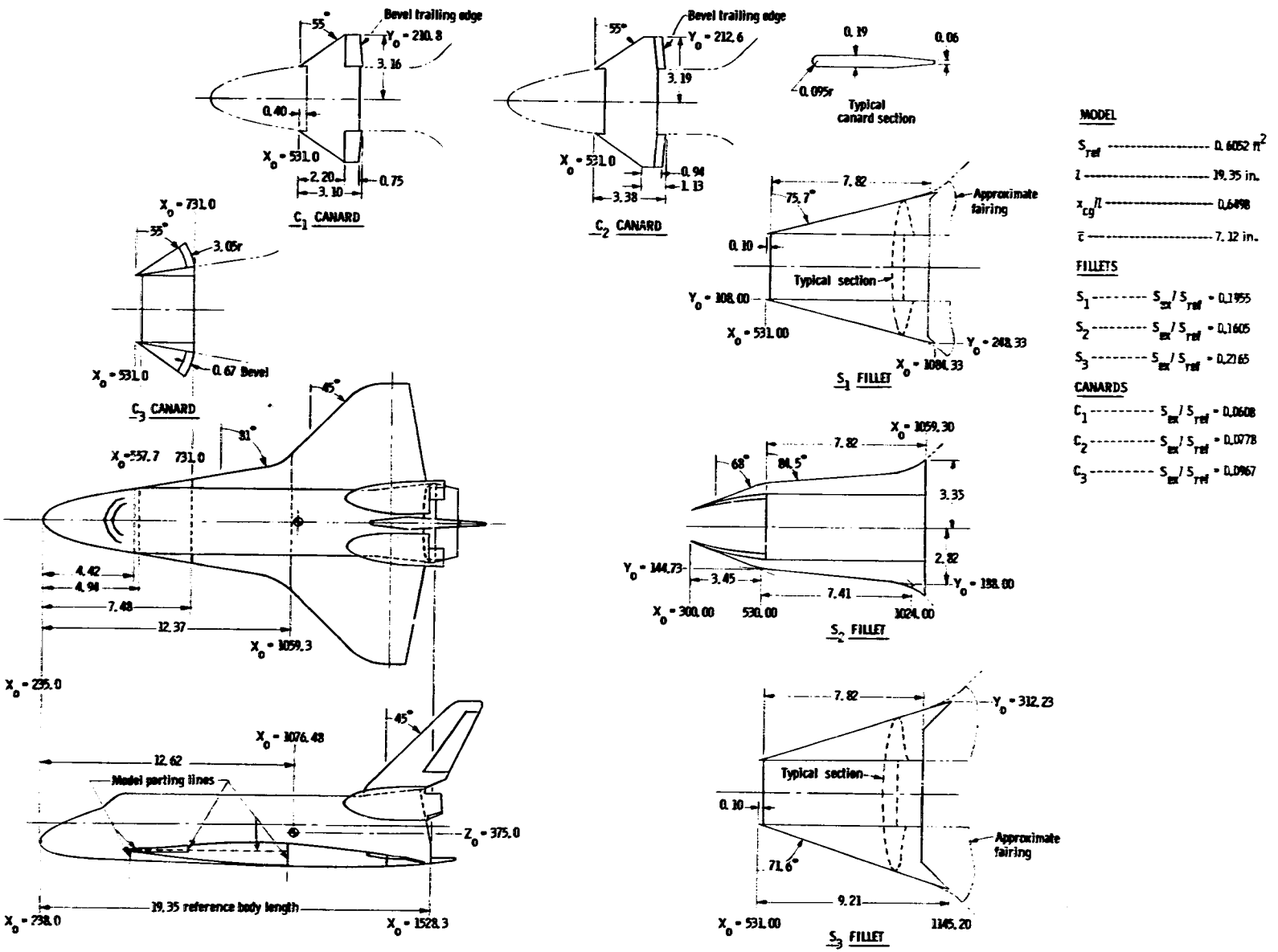

(a) Basic model, fillets, and canards.

Figure 5.- 0.015-scale 140A/B model and modifications. Dimensions in inches.

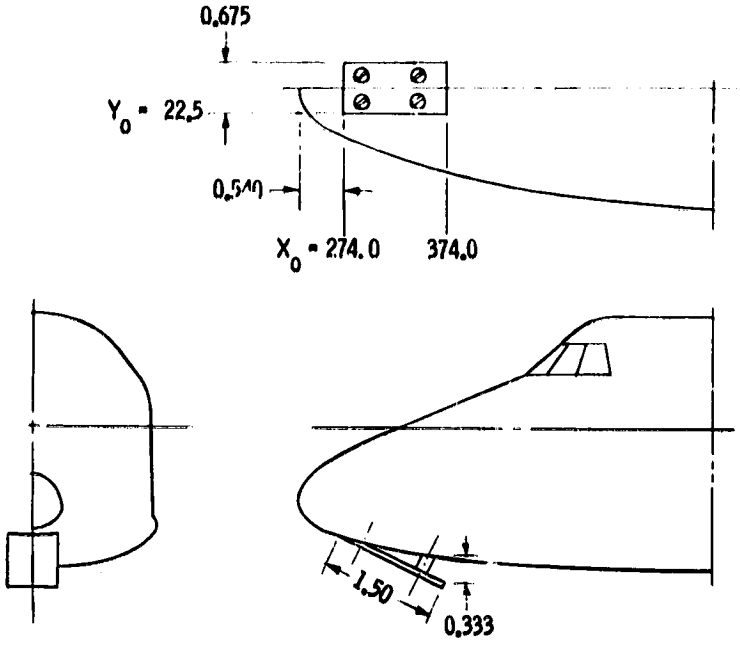

Nose-gear-door trim flap

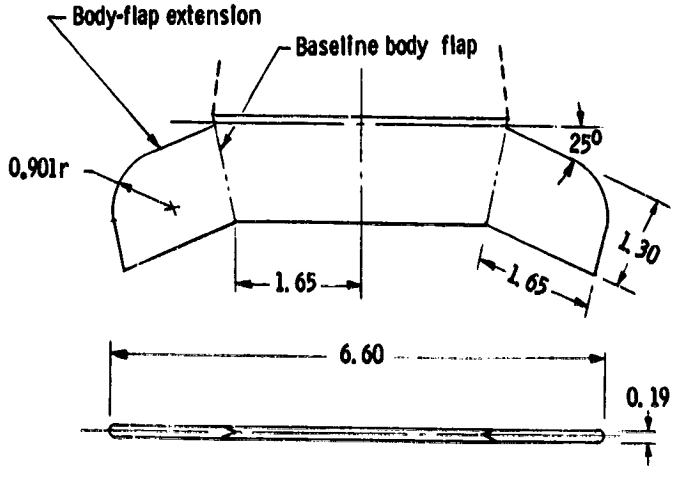

Extended-span body flap

(b) Nose-gear-door trim flap and extended-span body flap.

Figure 5.- Continued.

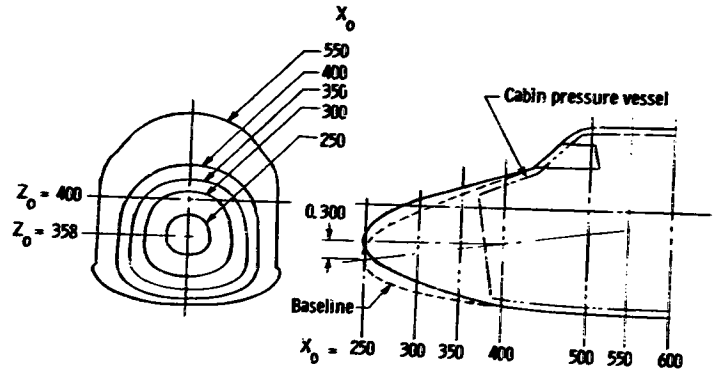

Minimum camber forebody, B_2

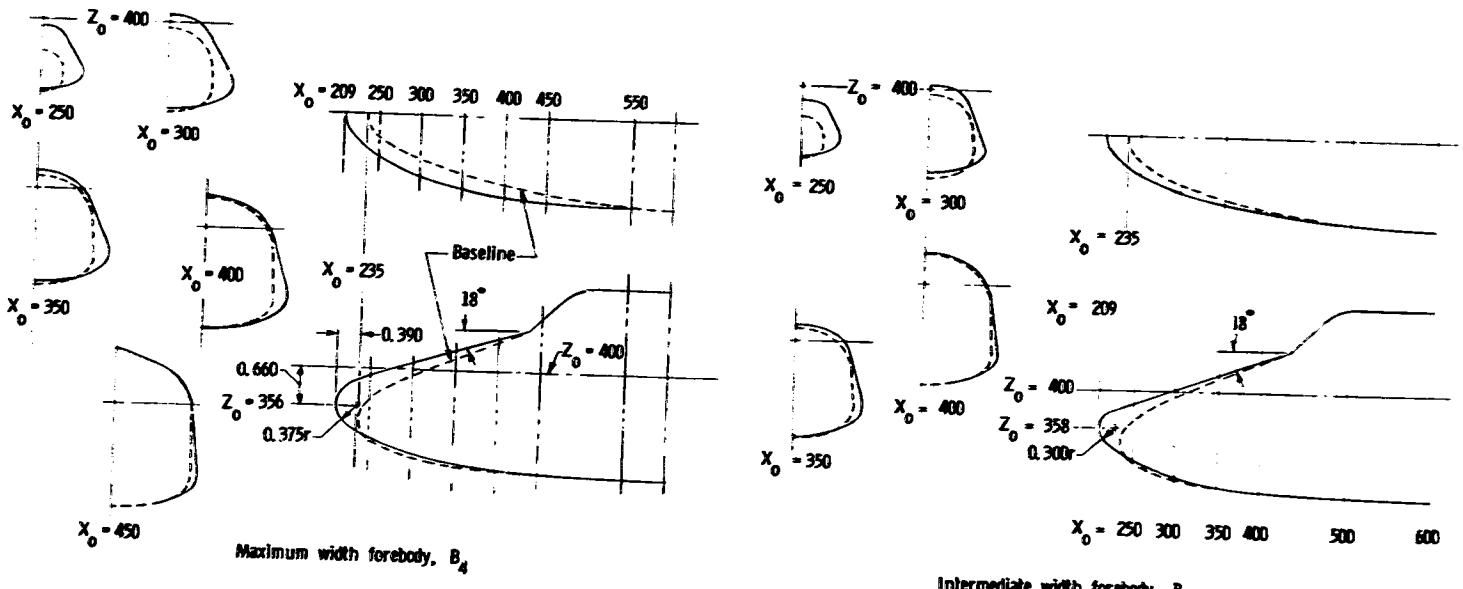

Maximum width forebody, B_4

Intermediate width forebody, B_5

(c) Forebody modifications.

Figure 5.- Concluded.

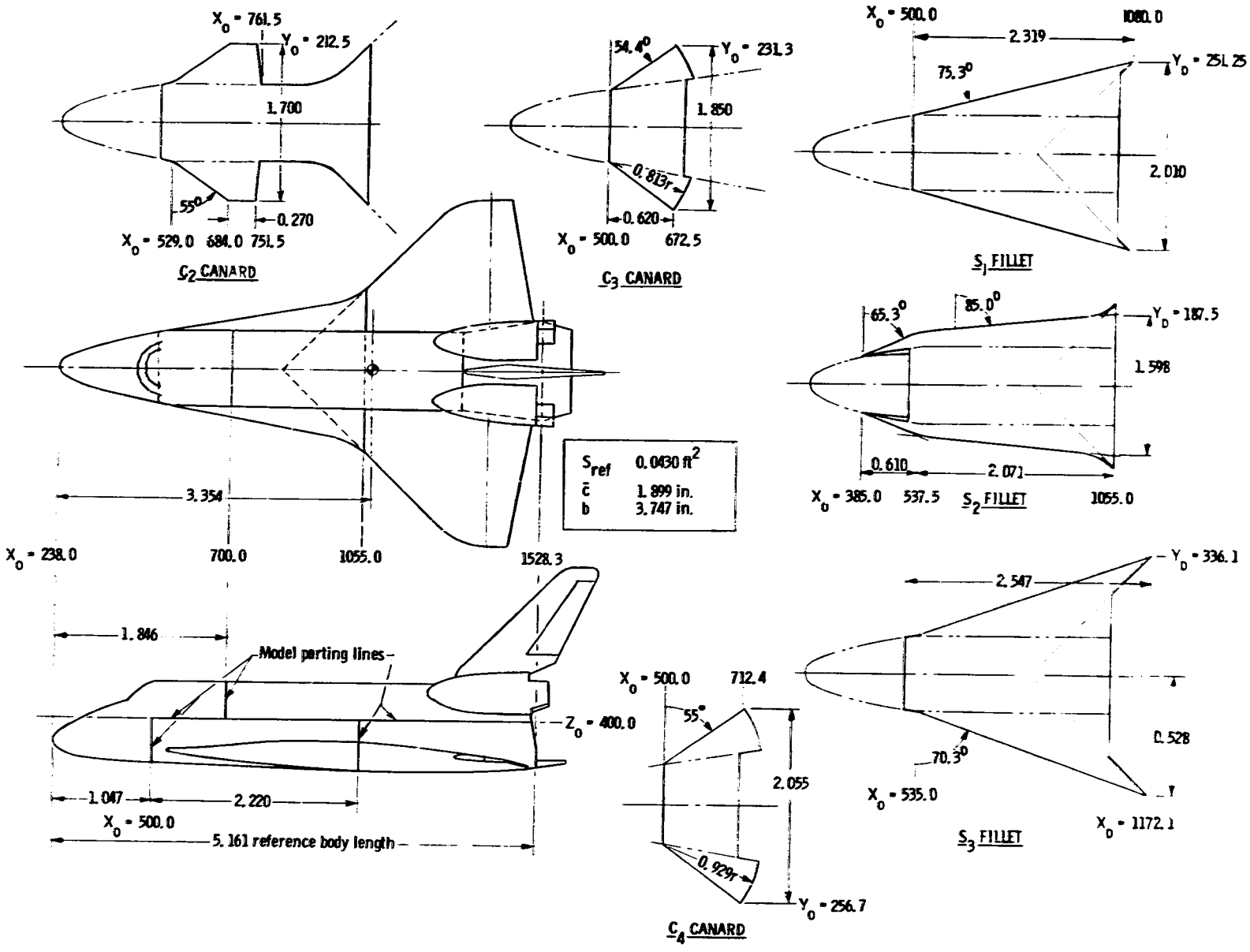

Figure 6.- 0.004-scale 139B model and modifications. Dimensions in inches.

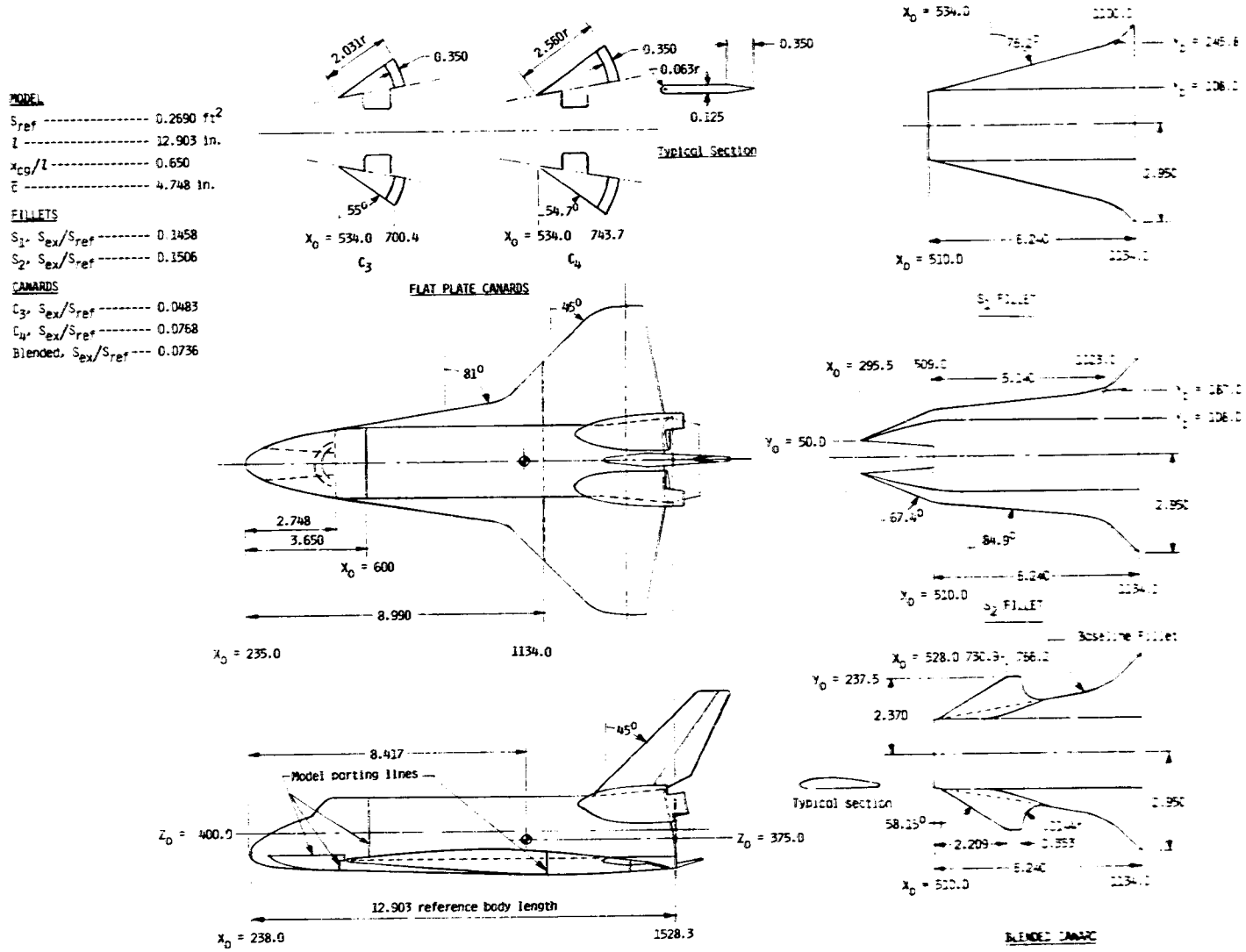

(a) Basic model, fillets, and canards.

Figure 7.- 0.01-scale 140A/B model. Dimensions in inches.

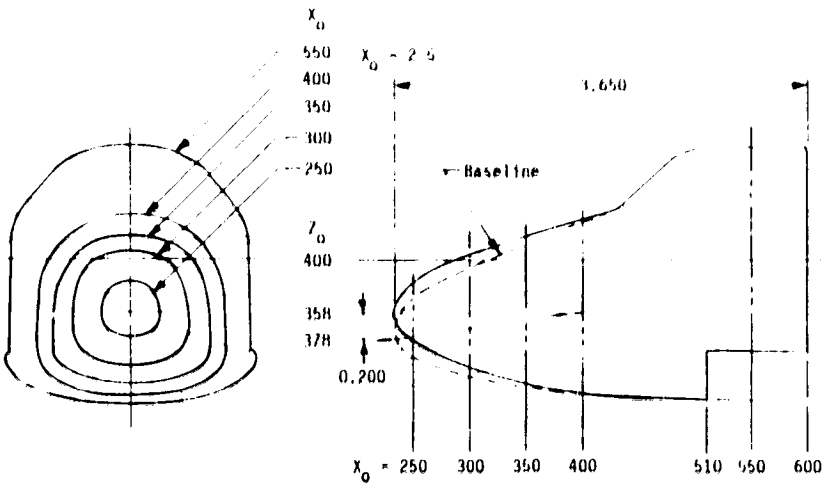

Minimum camber forebody, B_2

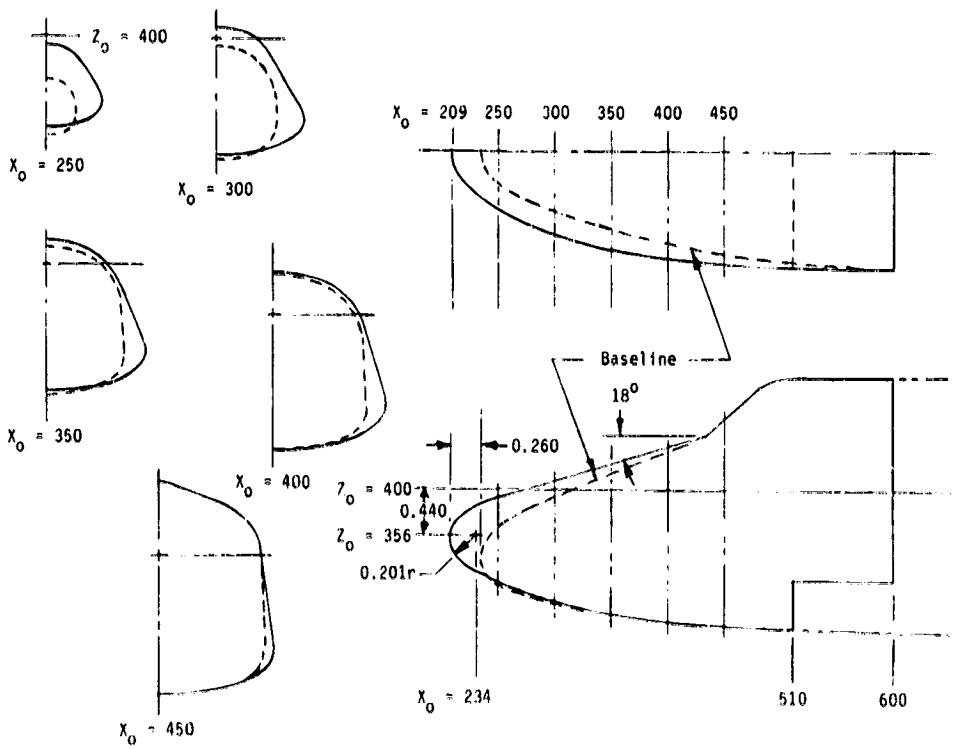

Maximum width forebody, B_4

(b) Forebody modifications.

Figure 7.- Concluded.

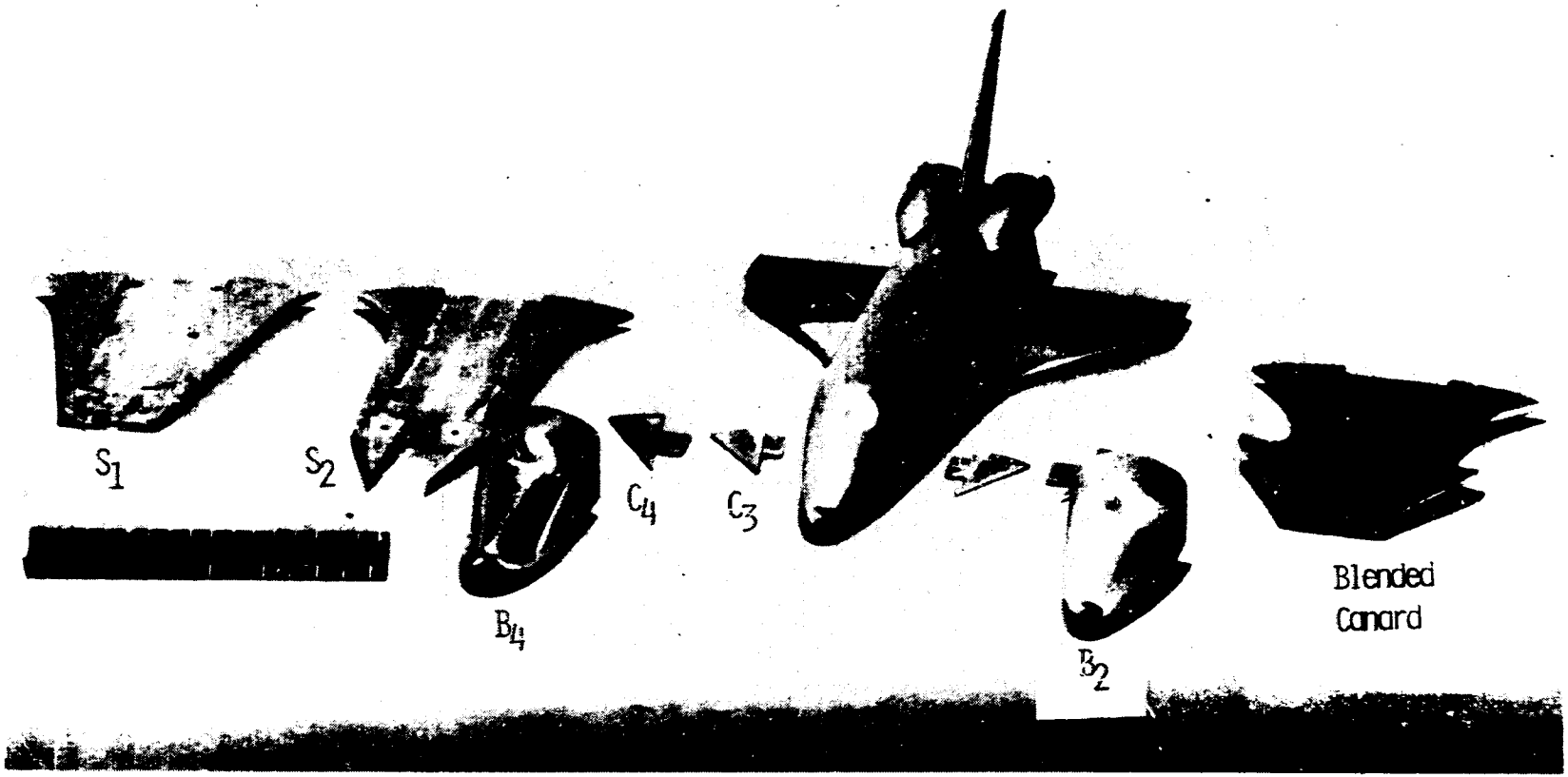

Figure 8.- Photograph of 0.01-scale 140A/B orbiter model.

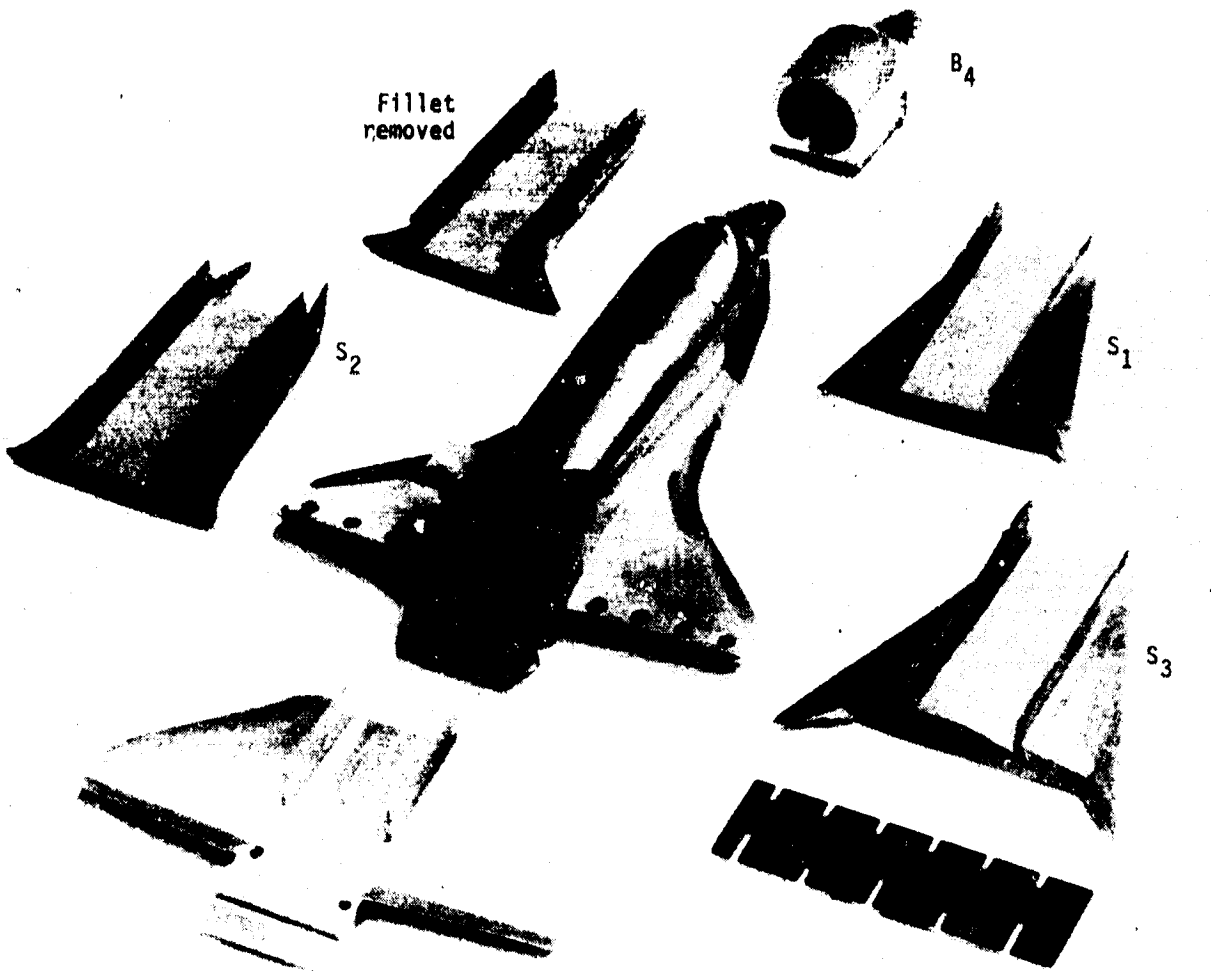

L-74-3864.1

(a) Fillet and forebody modifications.

Figure 9.- Photographs of the 0.004-scale 139B orbiter model.

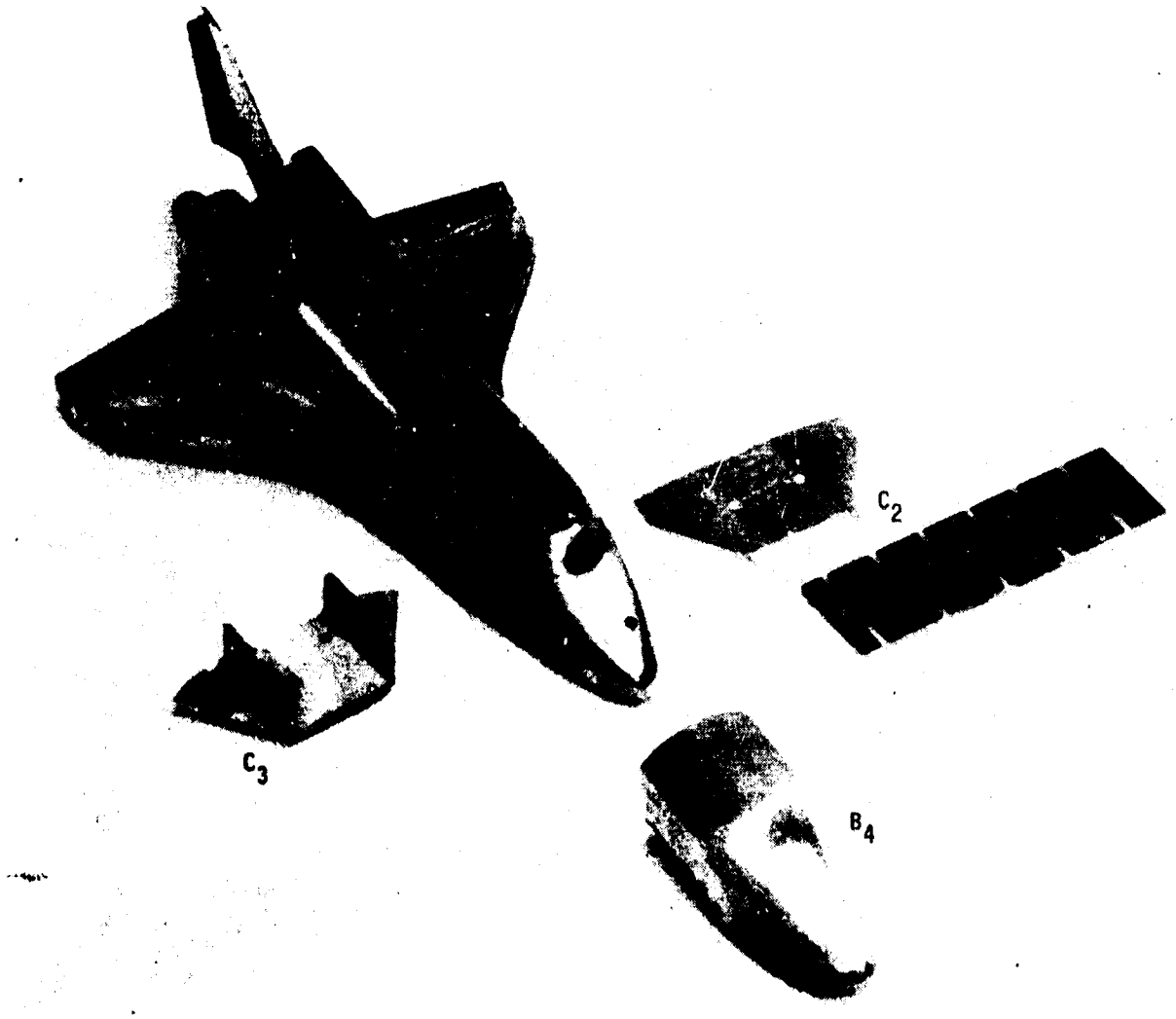

L-74-3863.1

(b) Canards and forebody modifications.

Figure 9.- Concluded.

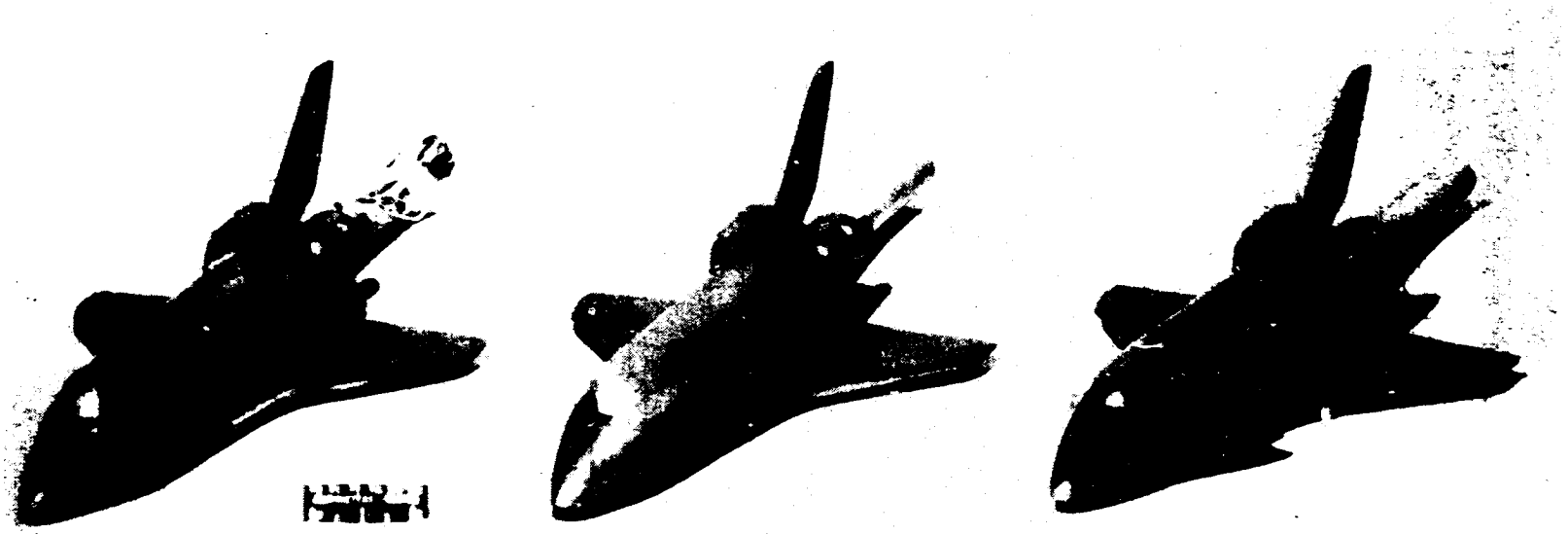

L-75-4017.1

Figure 10.- Photograph of the 0.01-scale 140A/B heat-transfer models.

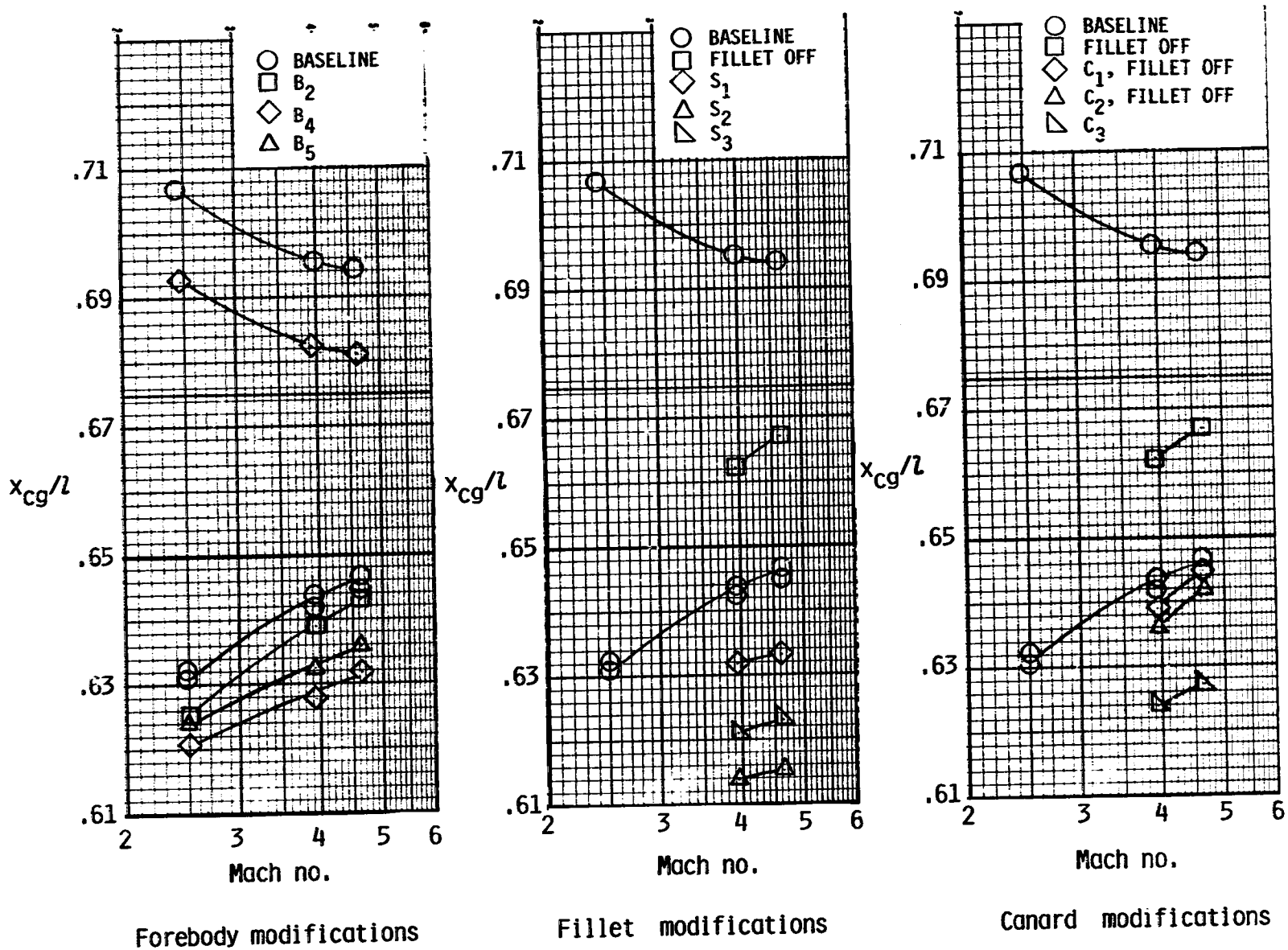

Figure 11.- Effect of modifications on supersonic trim c.g. capability from preliminary studies with the 0.015-scale orbiter model.

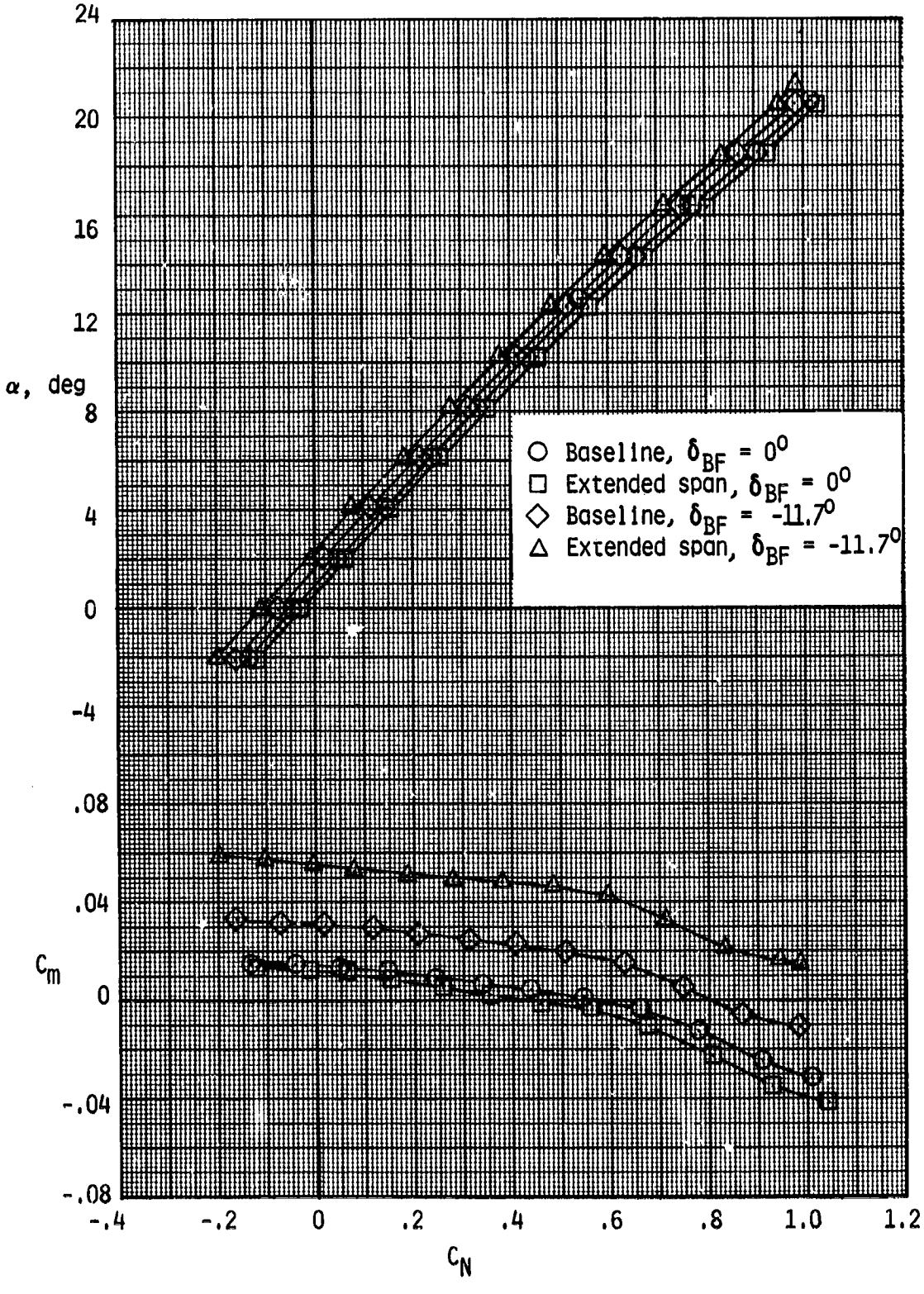

Figure 12.- Effect of extending body-flap span at subsonic speeds. M = 0.35; δ_e = 0°; 0.015-scale 140A/B scale model.

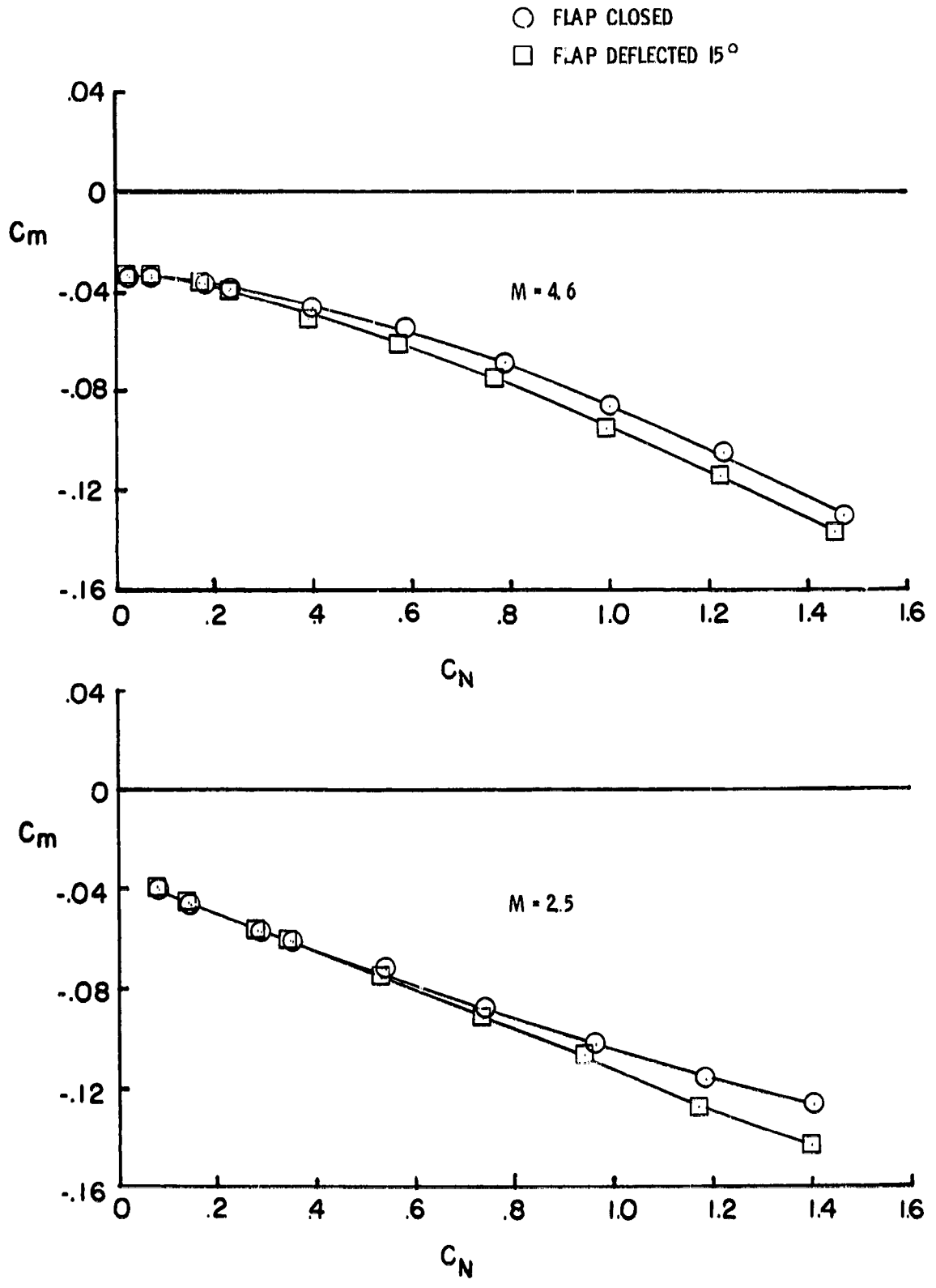

Figure 13.- Effect of nose-gear-door trim flap on supersonic trim capability.

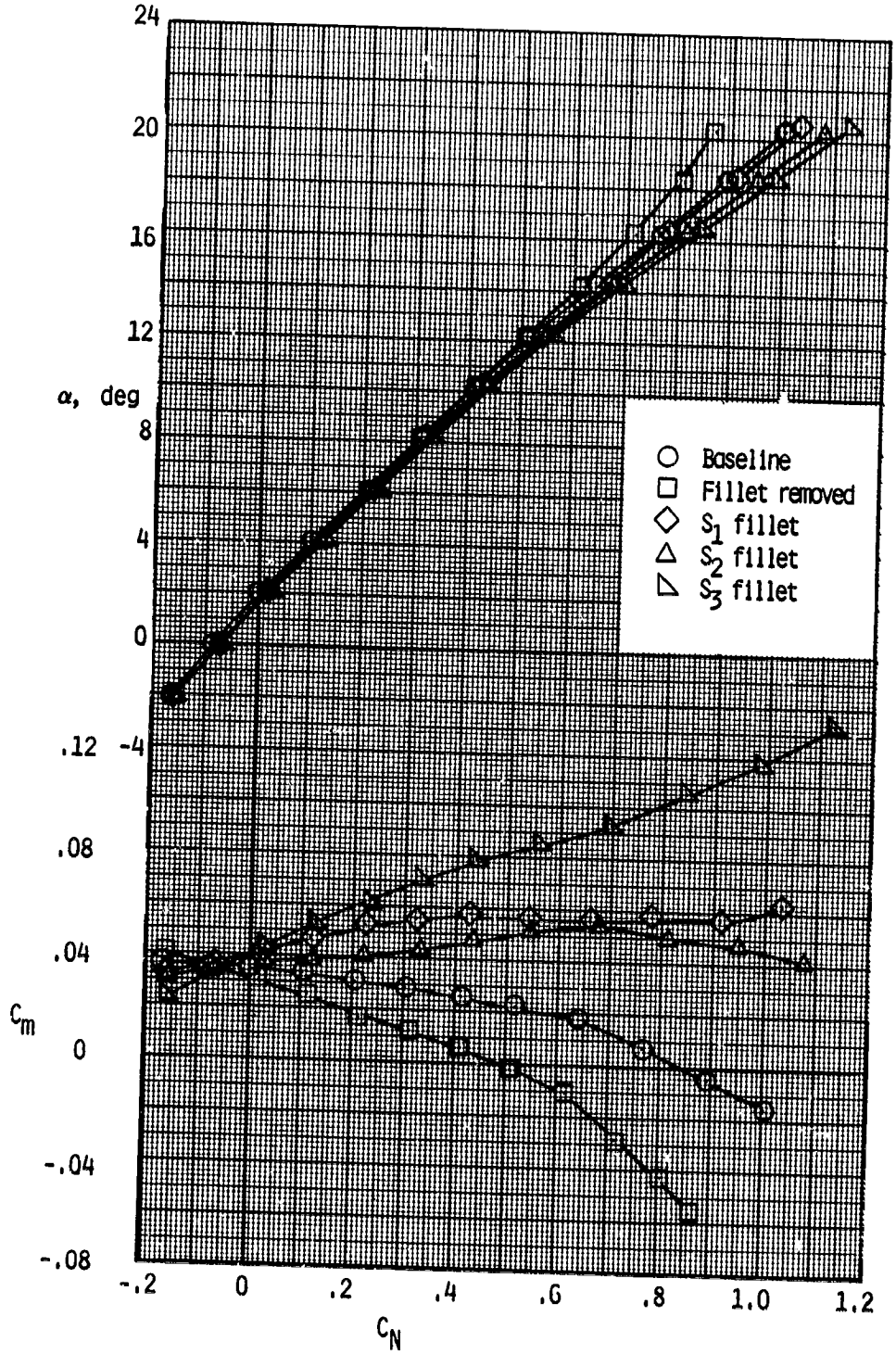

Figure 14.- Effect of fillet shape at subsonic speeds. M = 0.35; δ_{BF} = -11.7°; δ_e = 0°; 0.015-scale 140A/B model.

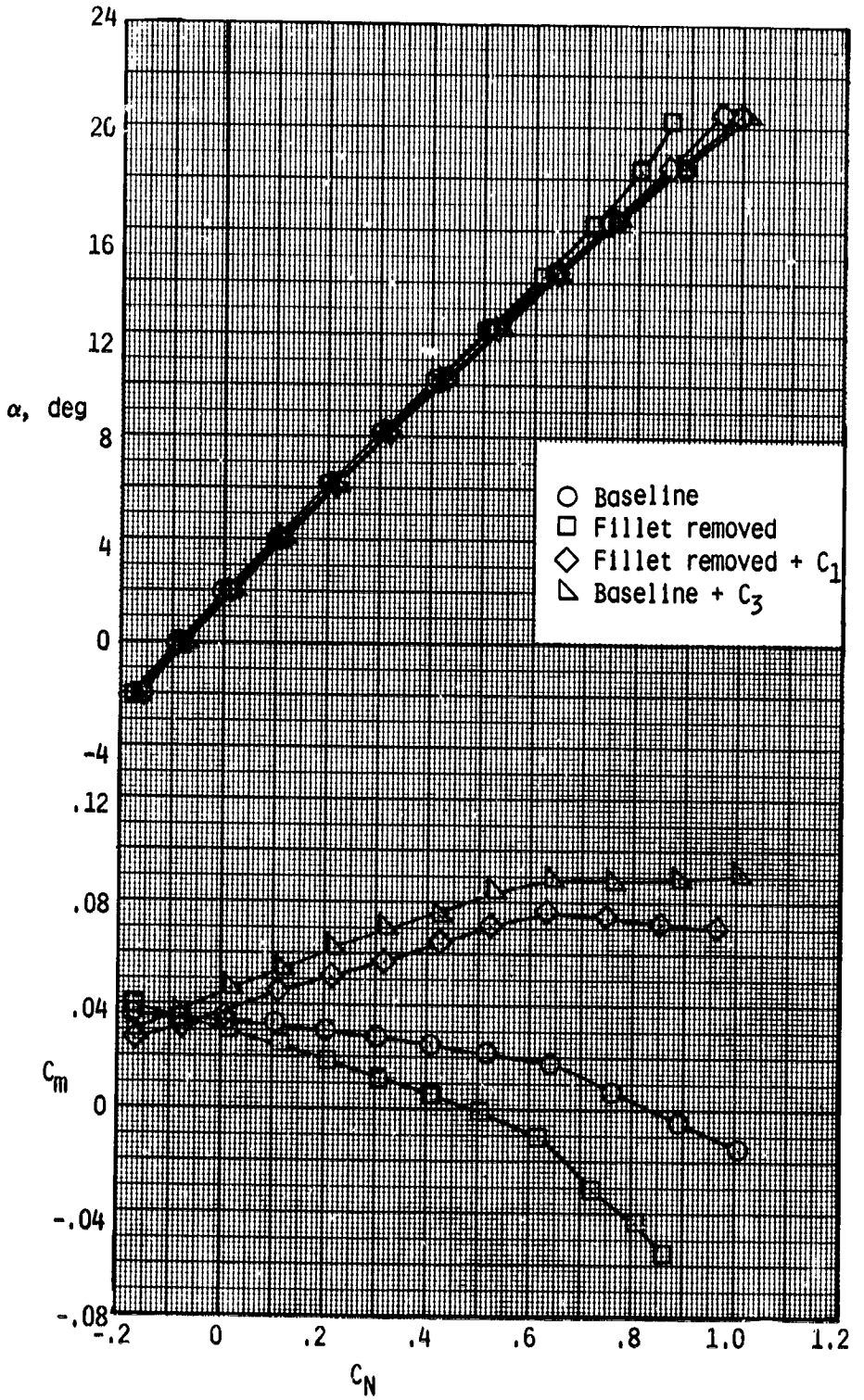

Figure 15.- Effect of canards at subsonic speeds. M = 0.35; δ_{BF} = -11.7°; δ_e = 0°; 0.015-scale model.

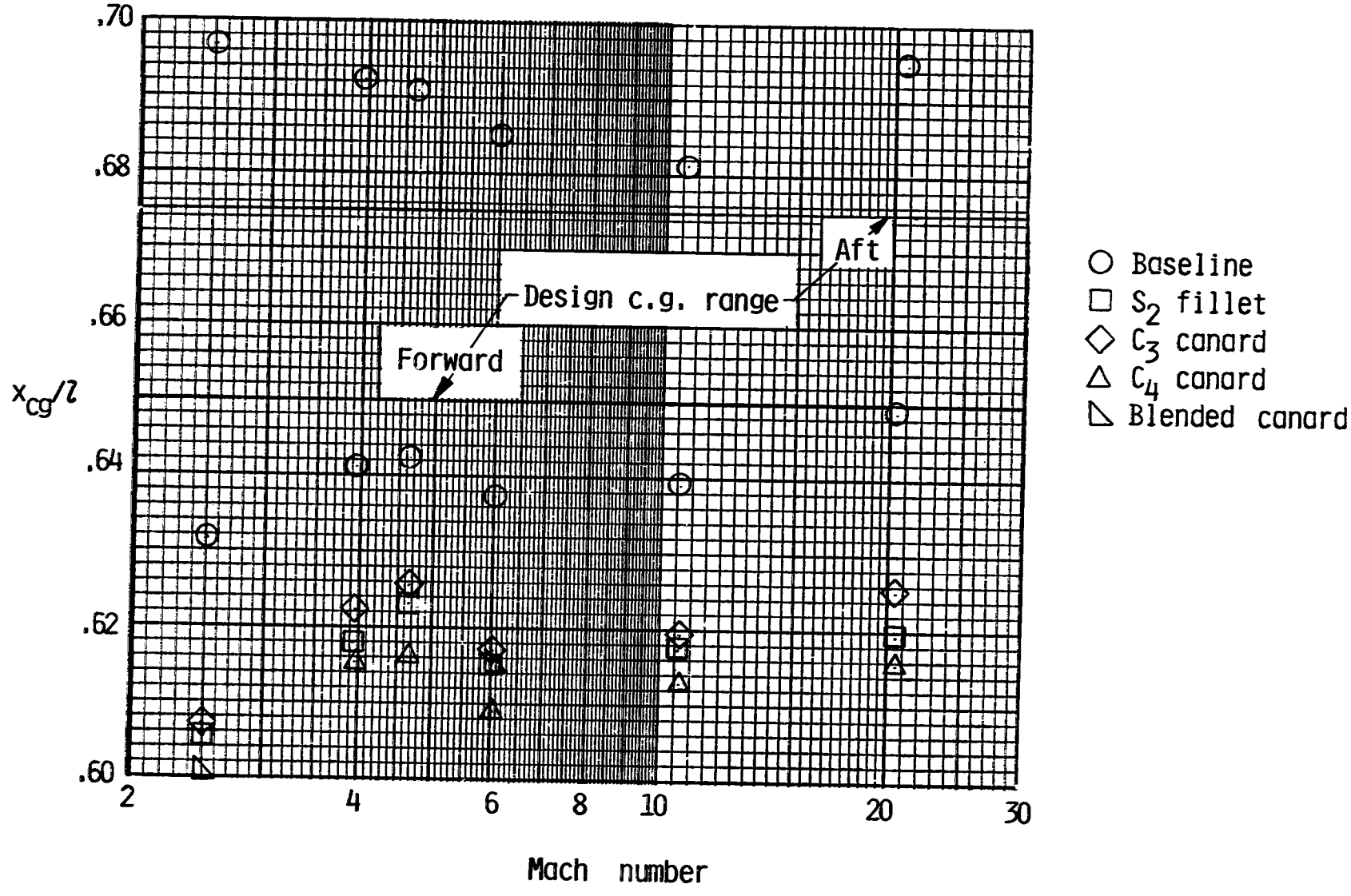

Figure 16.- Summary of orbiter supersonic and hypersonic trim forward c.g. capability with fillet and canards as determined with 0.01-scale 140A/B model.

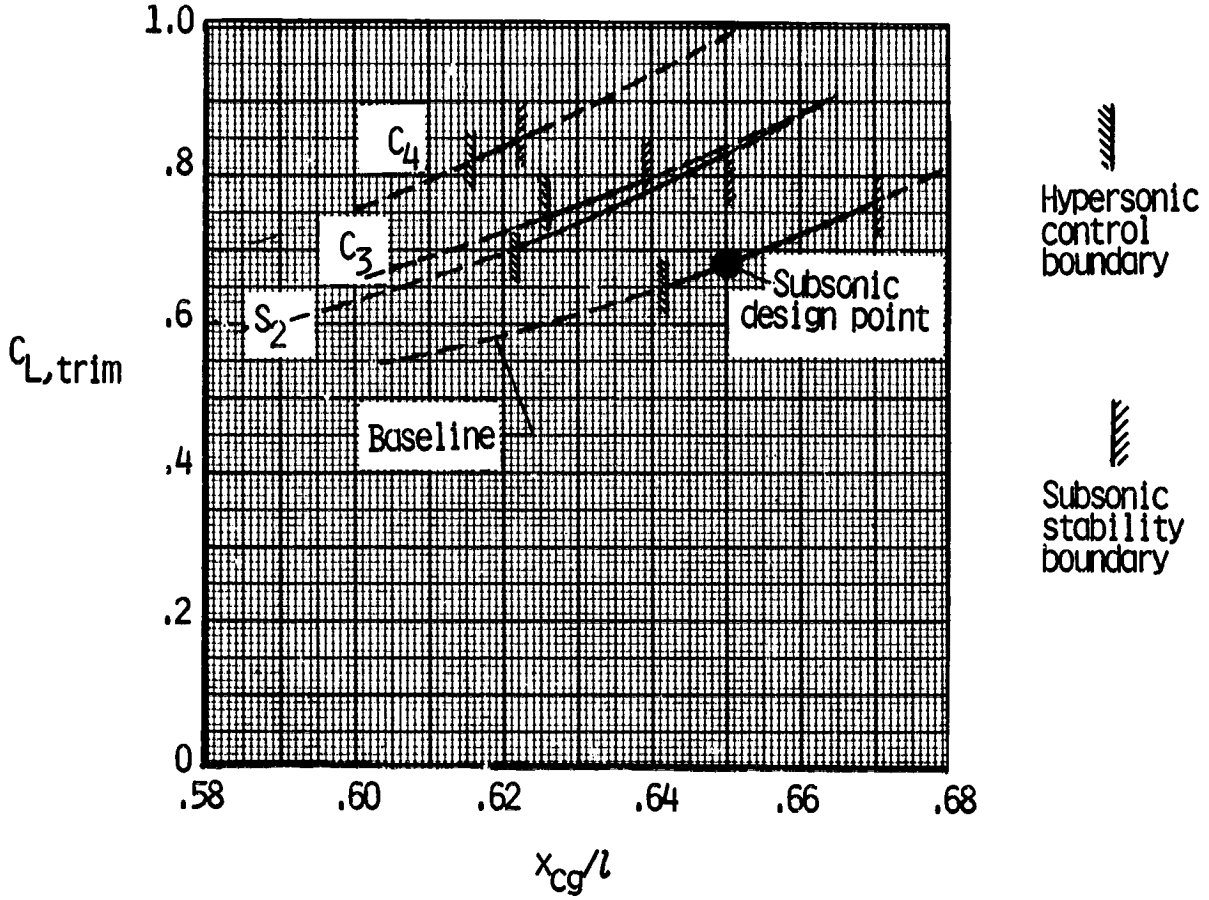

Figure 17.- Summary of orbiter subsonic longitudinal trim characteristics with forward-extended fillet and two flat plate canards at $\alpha = 15°$ as determined with 0.01-scale 140A/B model.

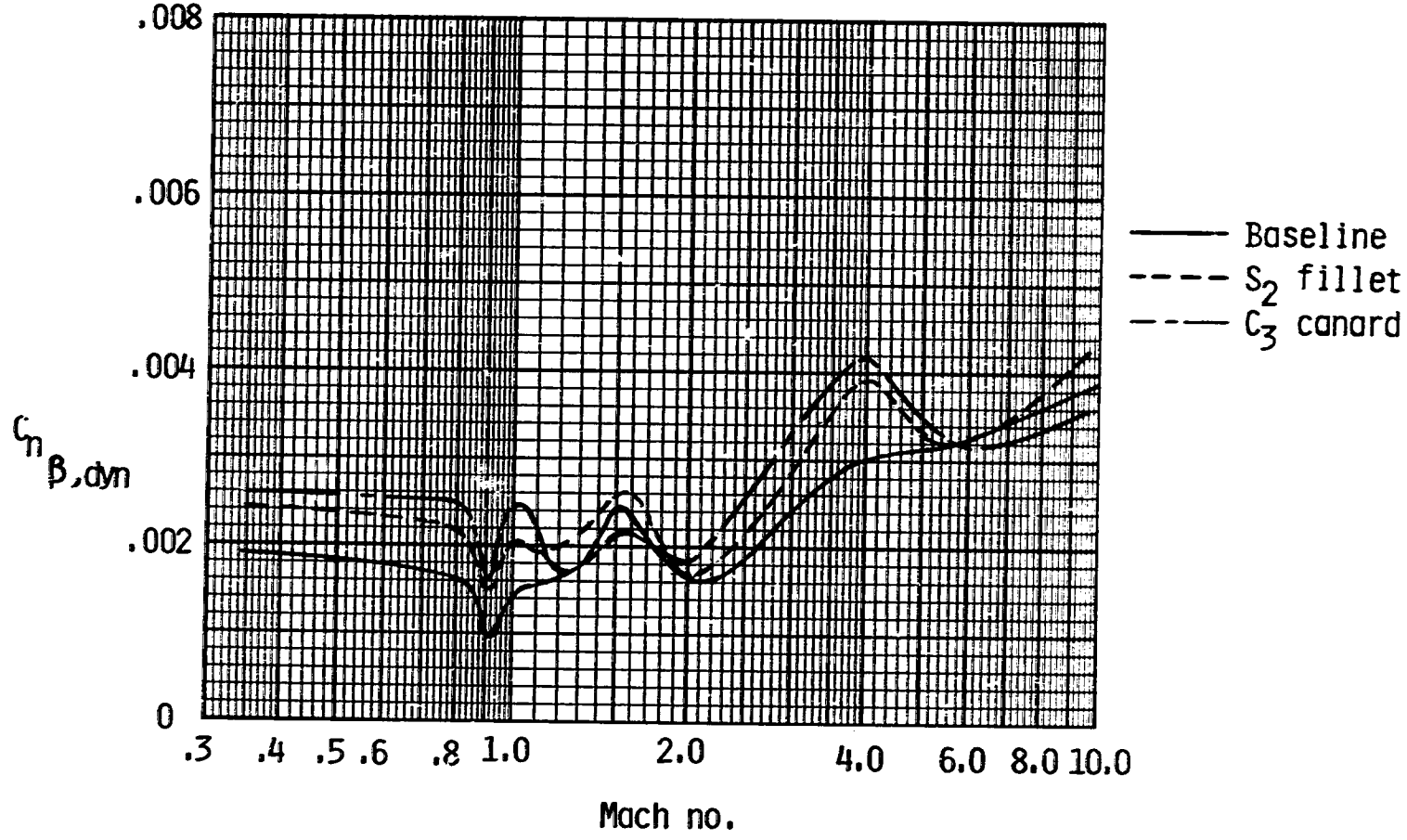

Figure 18.- Effects of fillet and canard modifications on lateral-directional stability parameter $C_{n_{\beta,dyn}}$ as determined with 0.01-scale 140A/B model.

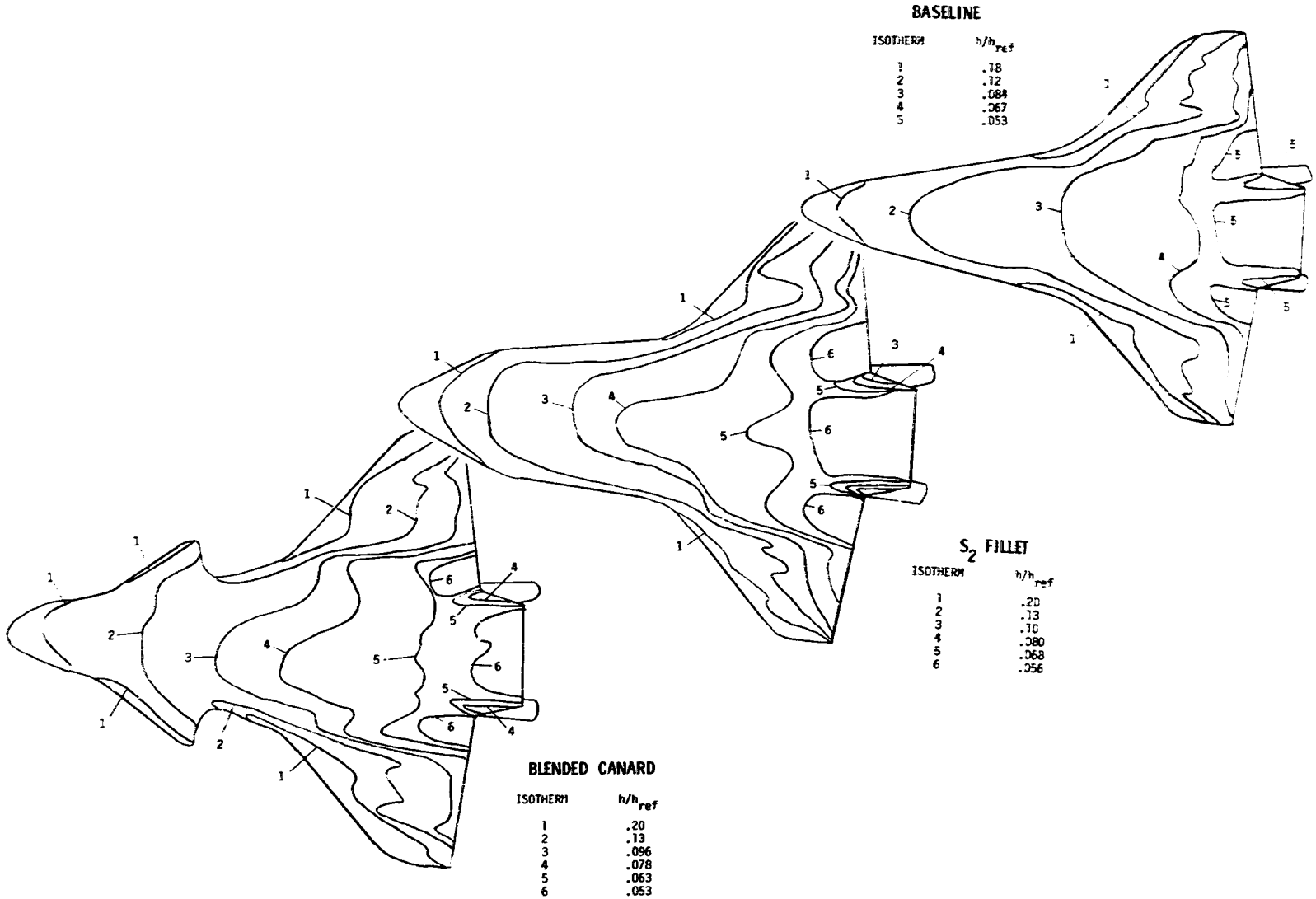

Figure 19.- Lower-surface heating contours for three configurations. $\alpha = 30°$; $R_l = 2 \times 10^6$. (From ref. 8.)

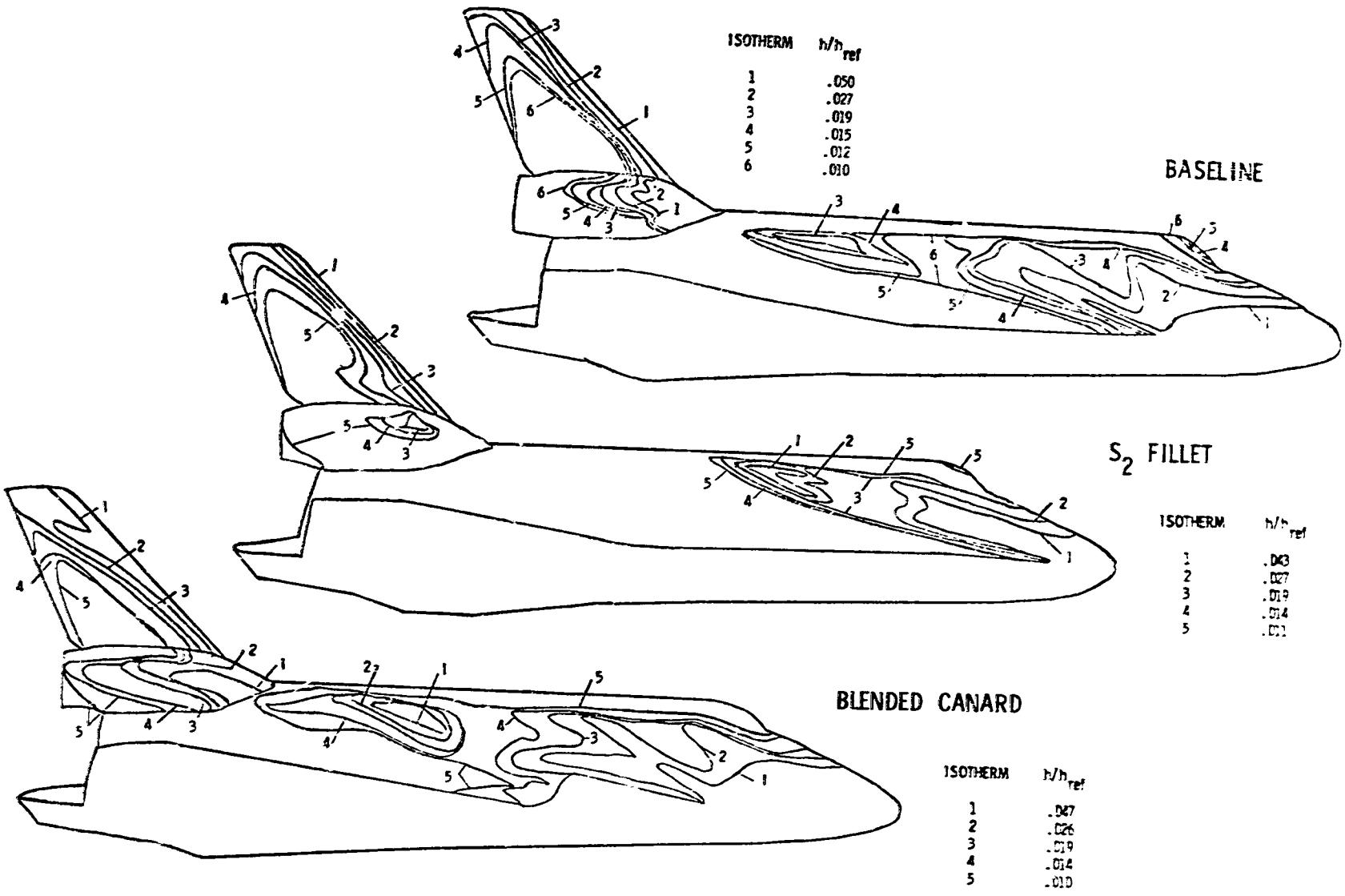

Figure 20.- Side heating contours for three configurations. $\alpha = 30°$; $R_l = 2 \times 10^6$. (From ref. 8.)

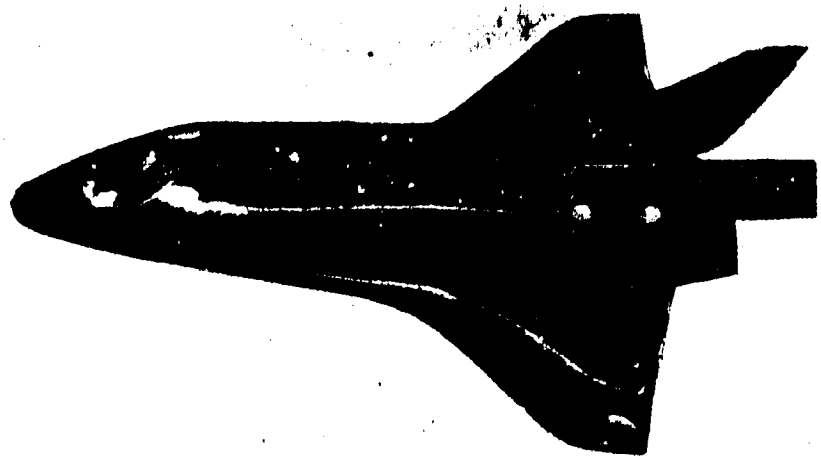

(a) Baseline.

(b) S_2 fillet.

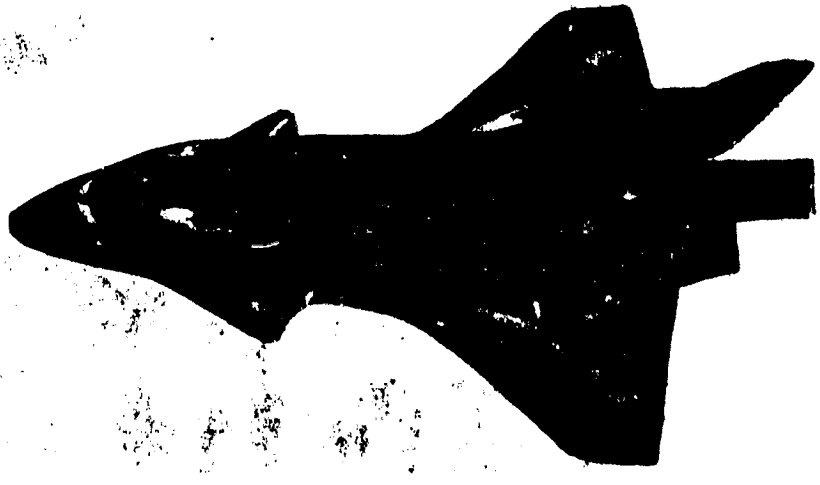

(c) Blended canard.

I-84-11

Figure 21.- Photographs of surface oil-flow patterns on orbiter model with baseline fillet, S_2 fillet, and blended canard as taken from reference 8. $\alpha = 30°$; $R_l = 1 \times 10^6$.

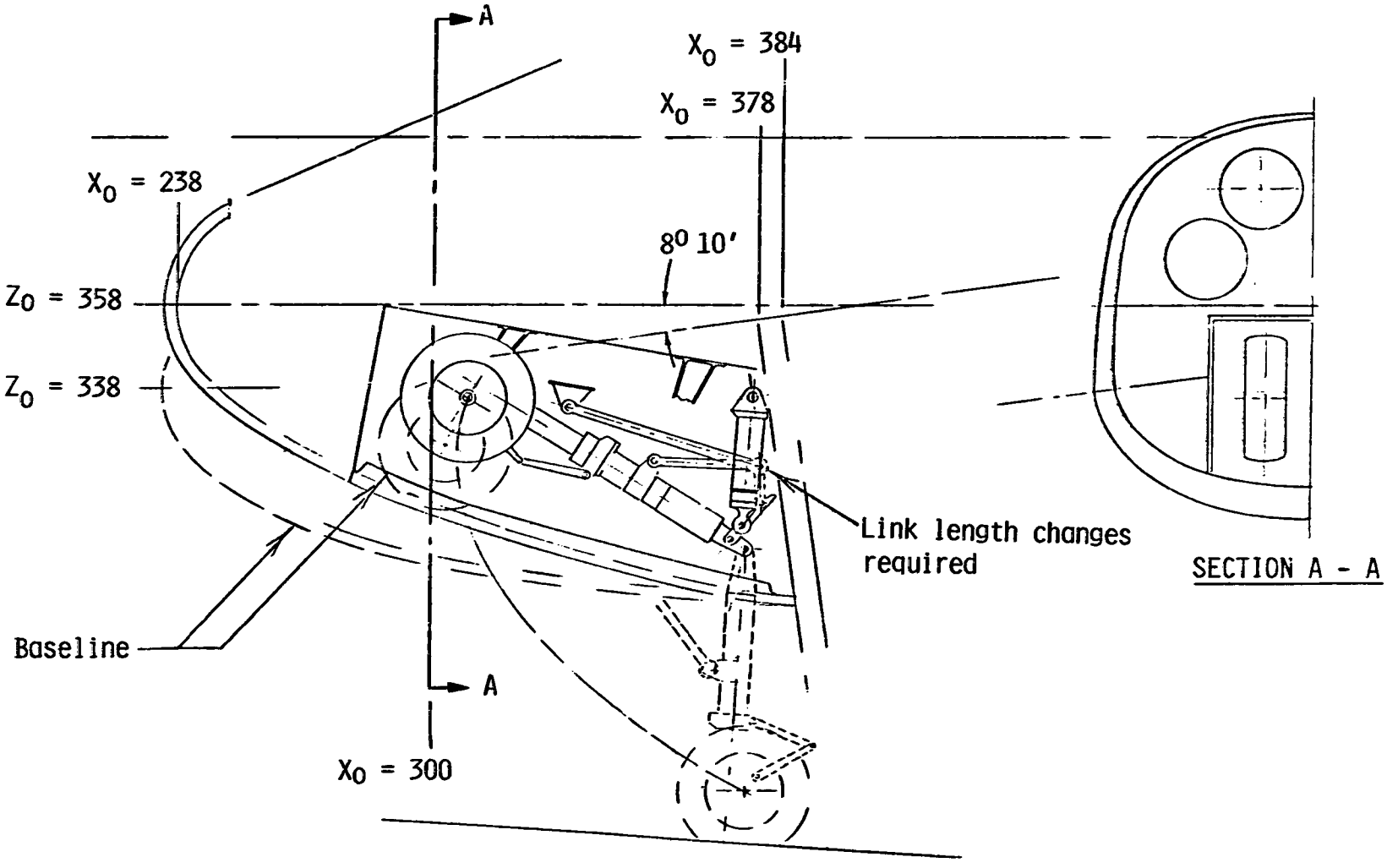

Figure 22.- Systems impact of minimum camber forebody, B_2, as taken from reference 9.

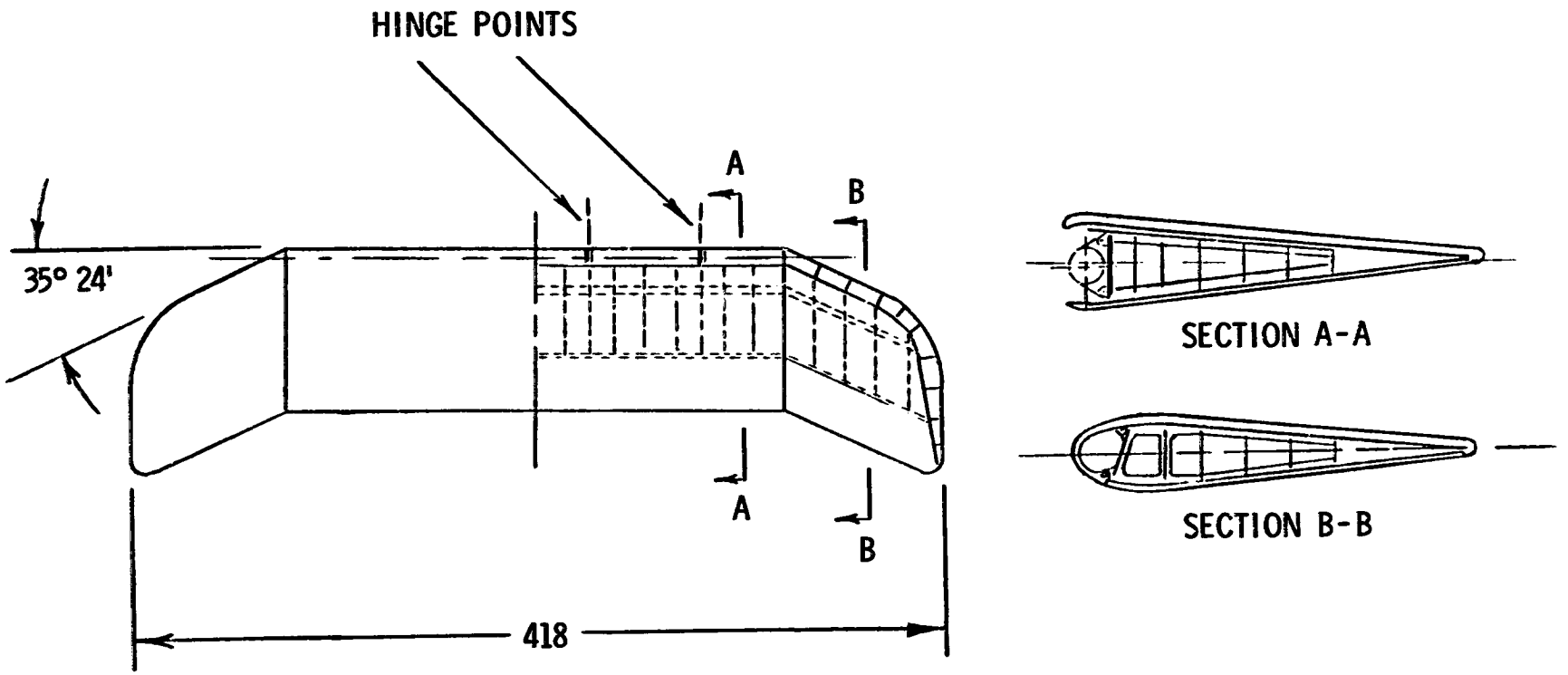

Figure 23.- Extended body-flap design from reference 9. Linear dimension in inches.

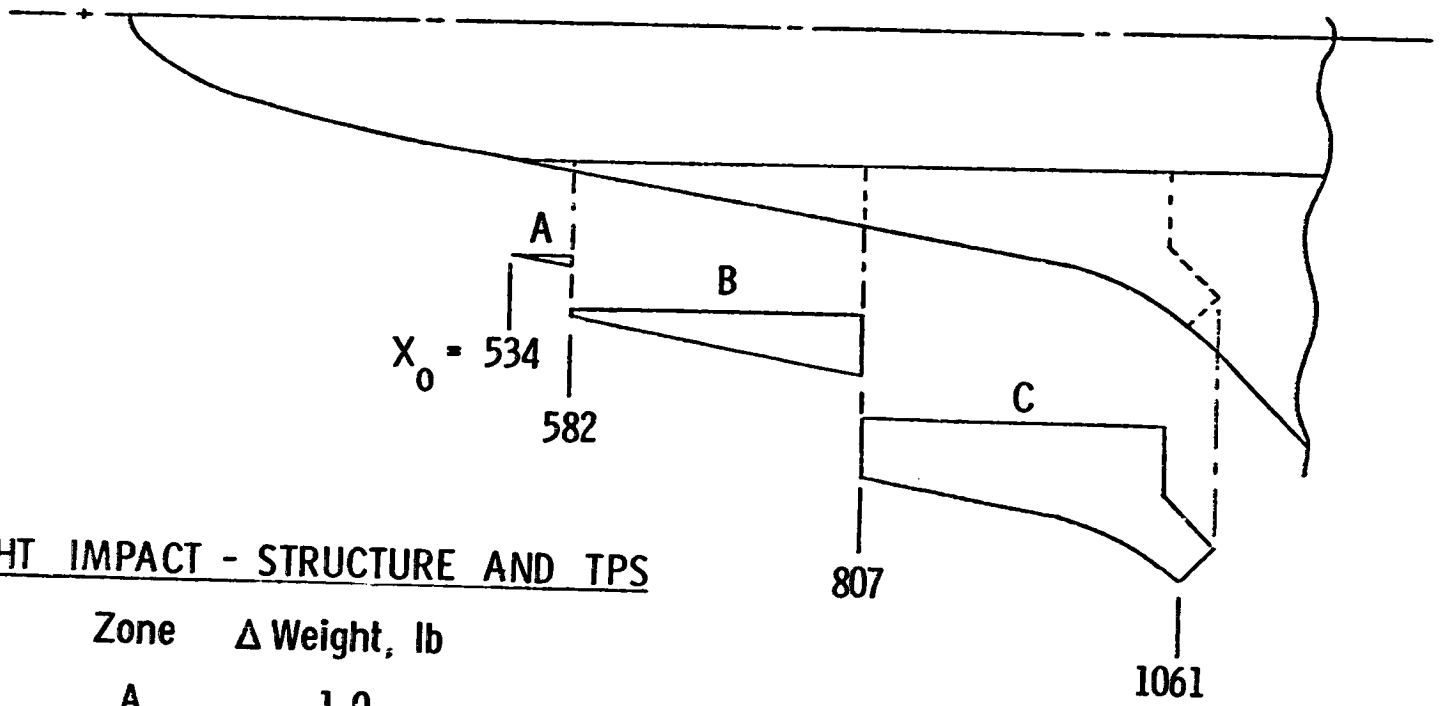

WEIGHT IMPACT - STRUCTURE AND TPS

Zone	Δ Weight, lb
A	1.0
B	40.0
C	70.0
Total	111.0

Figure 24.- Scar weight penalties for removable fillet. (From ref. 9.)

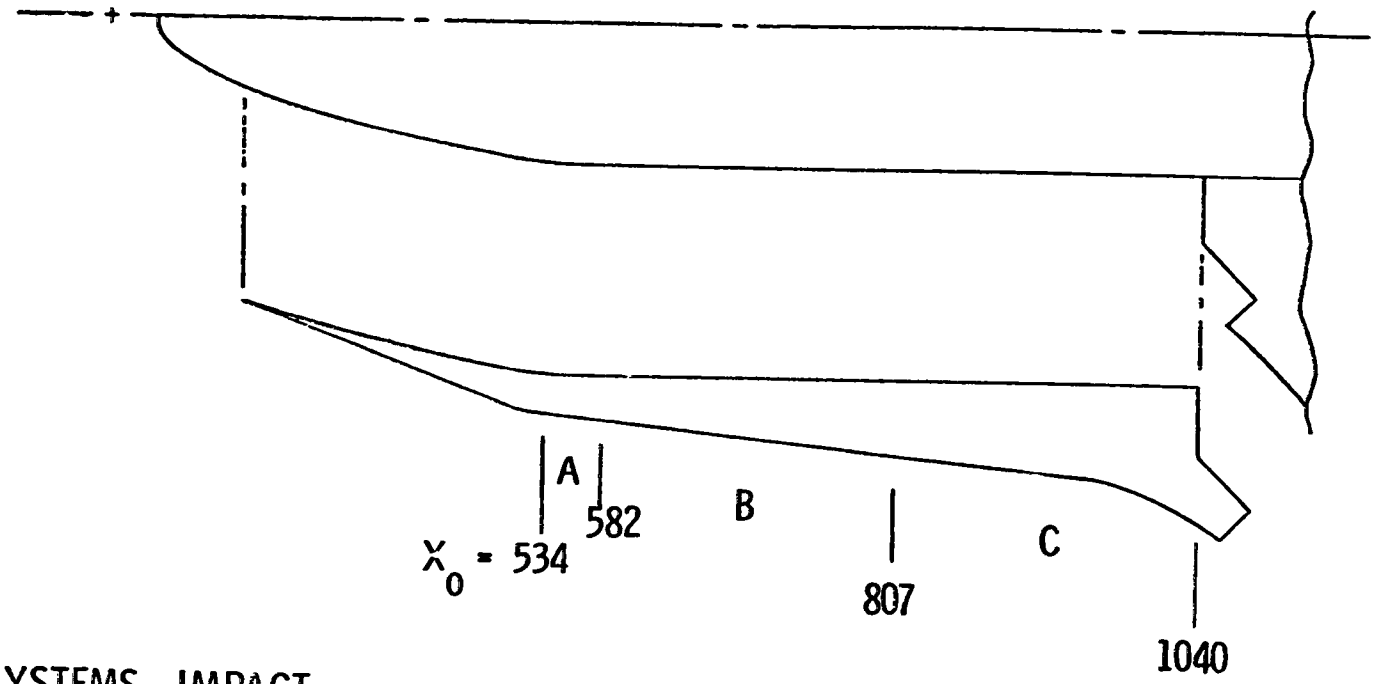

SYSTEMS IMPACT

Δ Weight = 1037 lb

Δ c.g. = 0.1 percent fwd

Δ Area = 134 ft^2

Figure 25.- S_2 fillet stations and mass properties impact. (From ref. 9.)

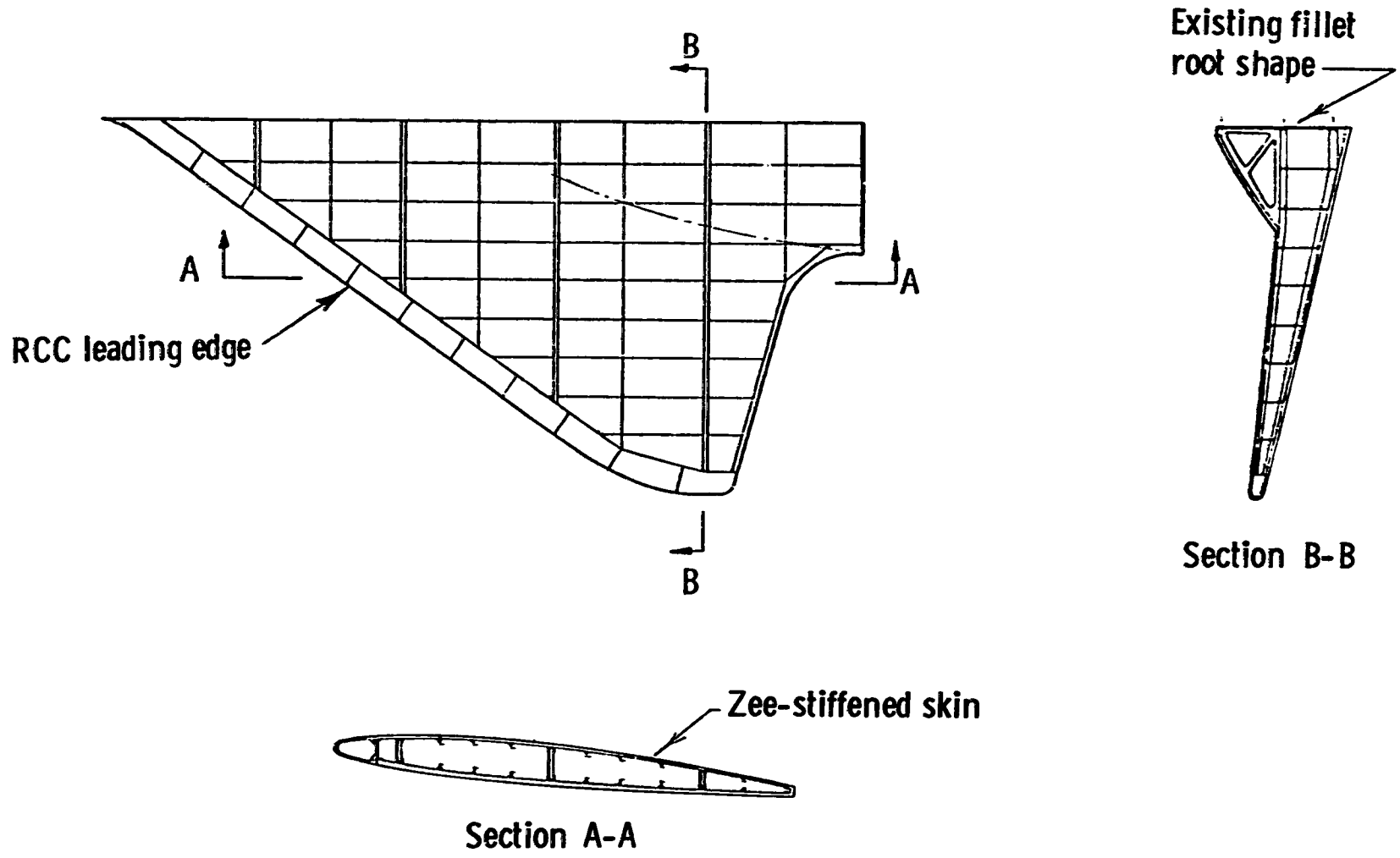

Figure 26.- Structural design concept for blended canard. (From ref. 9.)

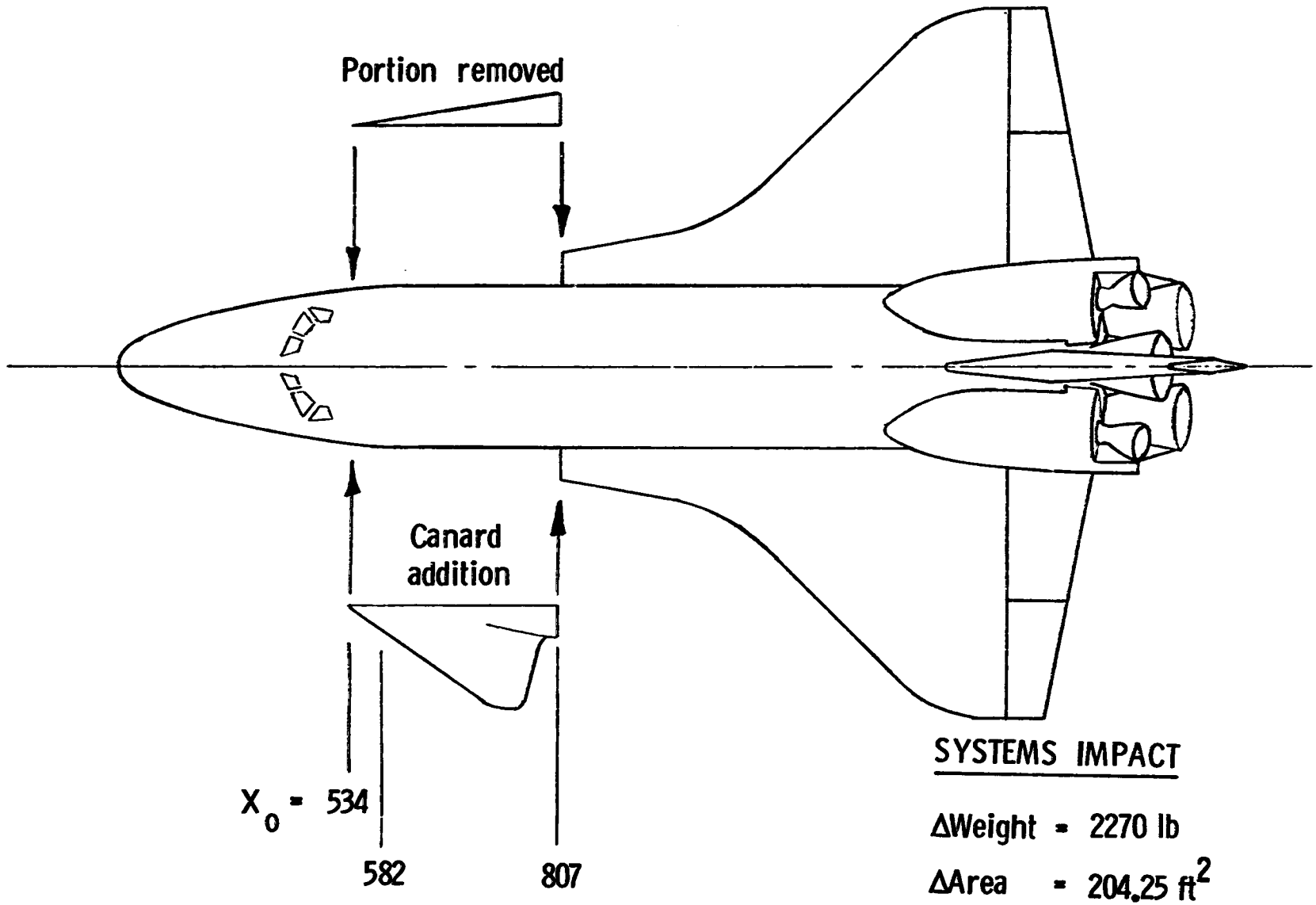

Figure 27.- System changes and station locations for blended canard design. (From ref. 9.)

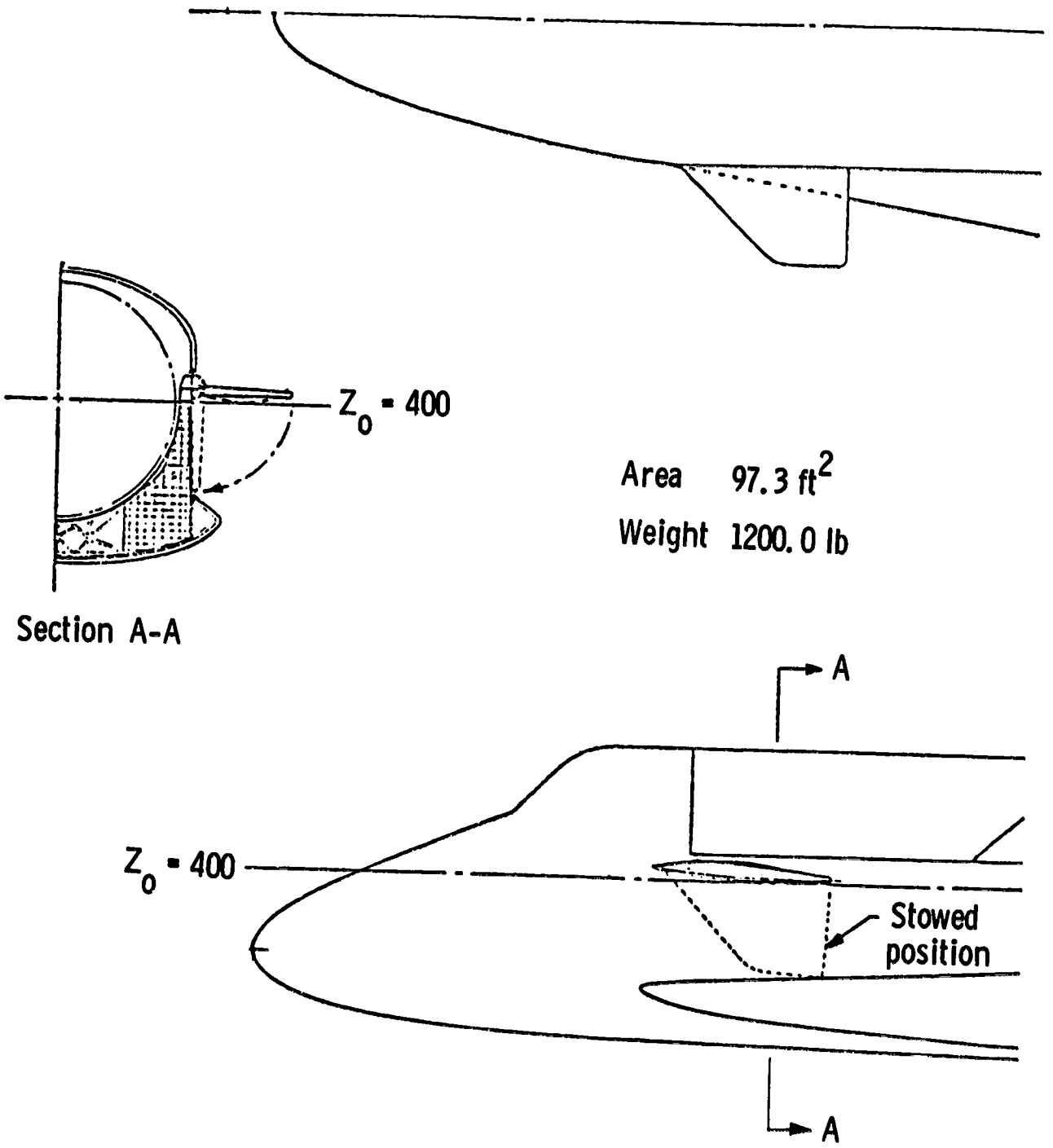

(a) Fold-down canard.

Figure 28.- Deployable canards studied in reference 9.

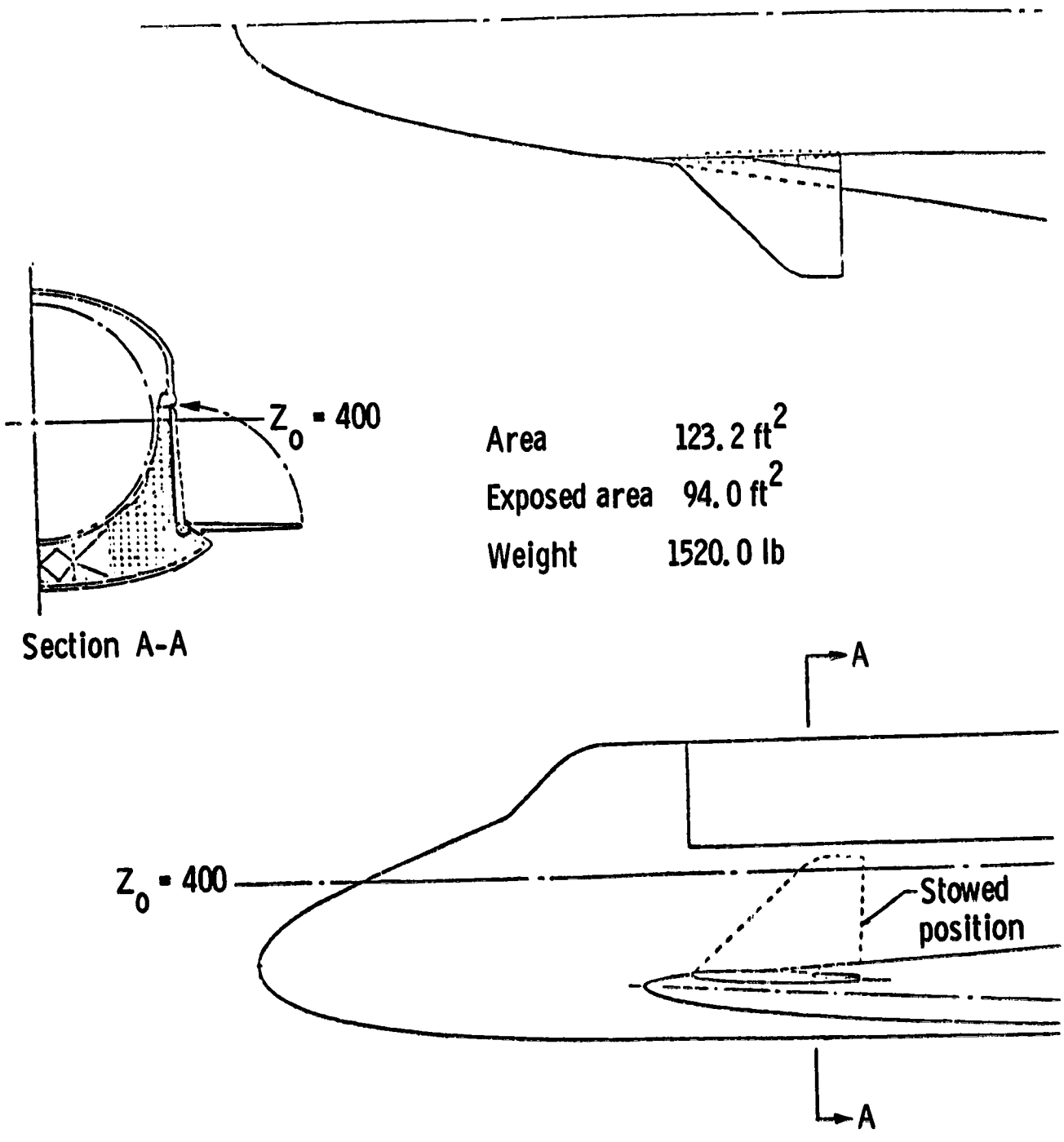

(b) Fold-up canard.

Figure 28.- Concluded.

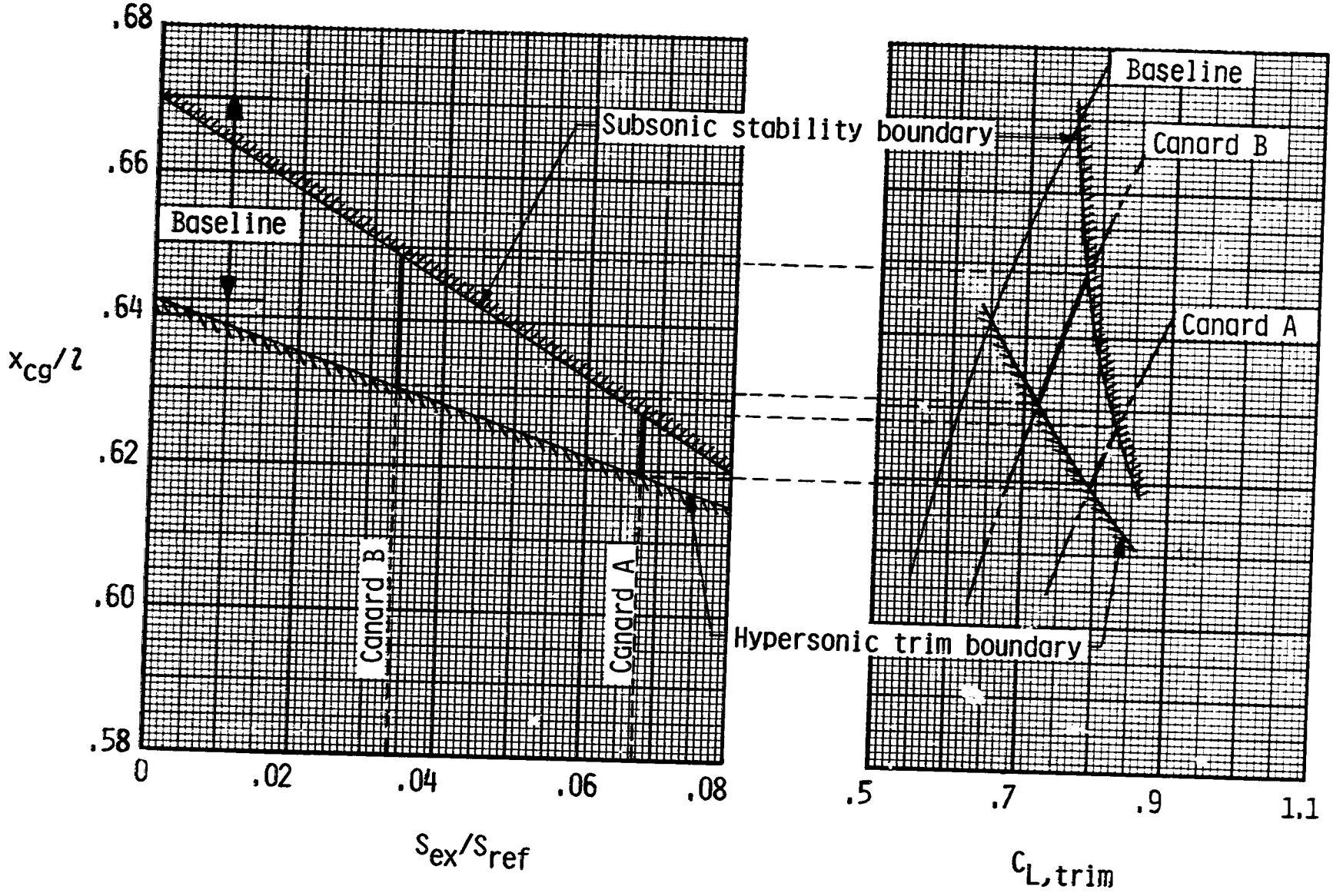

Figure 29.- Canard sizing nomograph.

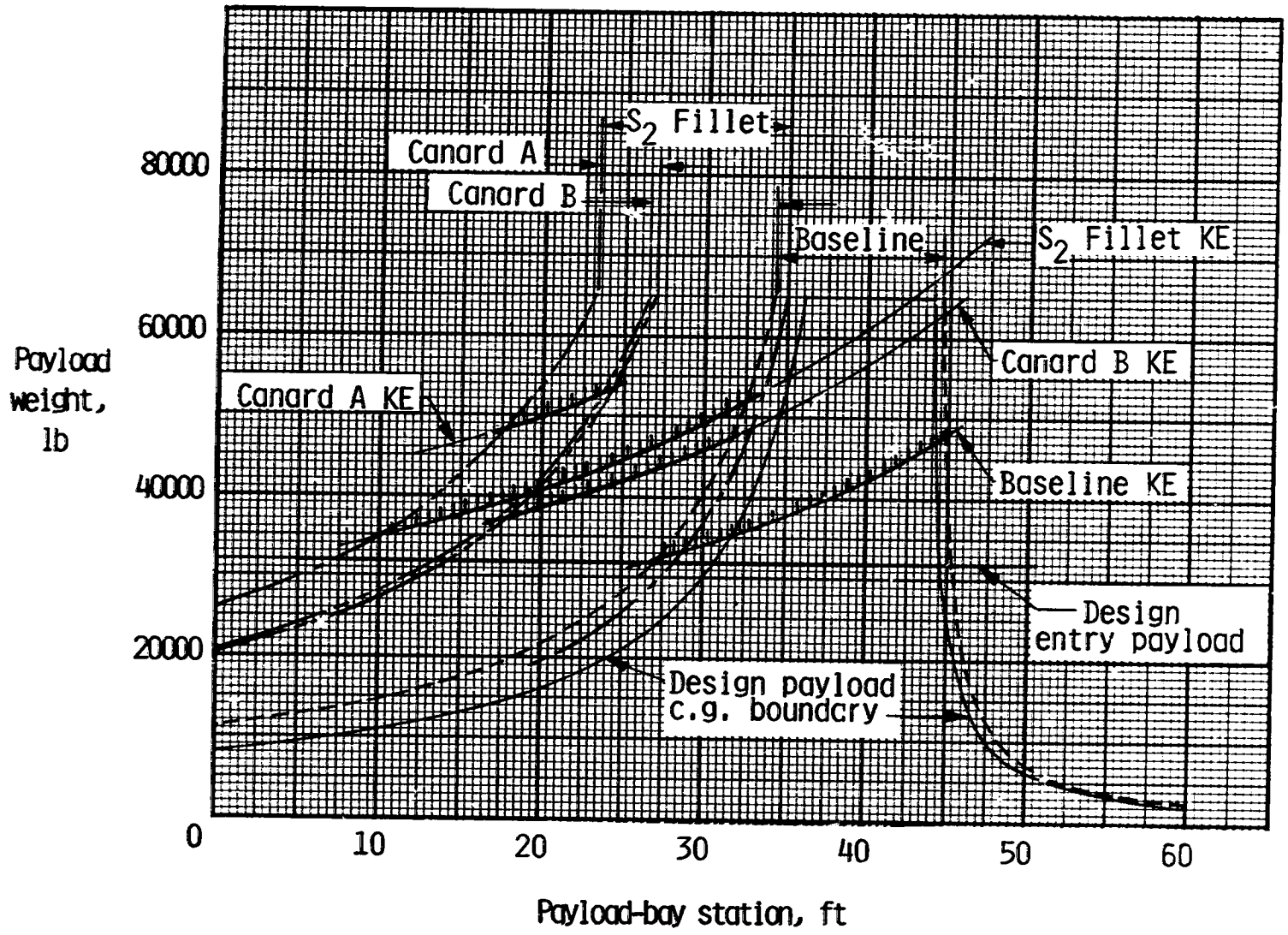

Figure 30.- Comparison of payload-bay c.g. envelopes of selected modifications with that of baseline flight-weight orbiter.